



Discover new correlations:

# The benefits of rheometry hyphenated with optical & spectroscopic techniques

Application compendium

# Introduction

## Material analysis with hyphenated rheometry

Current mega trends in society such as enhanced mobility, green energy, affordable healthcare and nutrition, etc. are driving the development of new materials. Smaller, lighter and self-healing materials are sought for automotive, aviation, coatings and many other industries. In the pharmaceutical industry for example, the bioavailability of new active ingredients and dosage forms has come into focus. In addition new functional food and cosmetics products are in constant need of enhanced analytical technology to meet tomorrow's consumer demands. All these market demands are driving researchers to look for a better understanding of new materials. They seek novel techniques that are easy to operate and help shorten the time to market for the next innovation. This is where rheometry hyphenated with spectroscopy or microscopy can answer the call.

## Discover new correlations – the benefit of hyphenating rheometry

Rheometry is the analytical method of choice to correlate the absolute flow and deformation characteristics of a given material with its behavior during specific processing or application steps. The data obtained represents the overall response of the material as it is exposed to the shear field in the measuring geometry. The mechanical properties of a material are directly related to its microscopic or molecular structure and structural changes. However, rheological measurements alone do not provide information about the structure and the changes that occur at the microscopic and/or molecular level. Combining rheometry with other analytical techniques provides the advantages of maximizing and synchronizing the data collected from individual experiments.

### Rheometry and microscopy

Combining rheometry with optical microscopy allows scientists to observe the change of a material's microstructure under shear deformation. This includes the investigation of droplet formation and coalescence in emulsions as well as aggregation and disaggregation of solid dispersions. When using adjustable polarization filters, crystallization processes can also be monitored, for instance, as a function of temperature. A high frequency stroboscopic light source allows for microscopic studies even at higher shear rates.

### Rheometry and Fourier Transformed Infrared (FTIR) spectroscopy

When combining rheometry with FTIR spectroscopy, the rheometer can be used for two purposes:

1. As a simple source of well-defined stress-deformation and temperature profiles. The simultaneously recorded spectra reveal shear induced molecular changes (e.g. stretching, orientation or rupture).
2. To monitor physical processes like chemical/thermal cross-linking and curing reactions. The area under the relevant peaks in the FTIR spectra can be determined and plotted together with the simultaneously acquired rheological data as a function of time or temperature, revealing, for example, reaction kinetics.

### Rheometry and Raman spectroscopy

Melting and crystallization are two common phase transitions that are critical to the flow properties of various complex fluids. These temperature-sensitive transitions are often indicated via changes in molecular conformation, which can be monitored using Raman spectroscopy. This is extremely useful for studying the crystallization behavior of polymer melts during different processing applications such as injection and blow molding or 3D printing.

Complementary methods such as those described above can offer a complete characterization of a specific sample. All of these hyphenated analytical techniques are possible with the Thermo Scientific™ HAAKE™ MARS™ Rheometer platform and its specialized accessories. Read more about the applications you can perform with this powerful analytical tool.

## Table of contents

### **Rheometry and microscopy**

- Investigation of pharmaceutical hot-melts via simultaneous rheometry and polarization microscopy
- Image acquisition at high shear rates via simultaneous rheometry and microscopy

### **Rheometry and Fourier Transformed Infrared (FTIR) spectroscopy**

- Curing of an acrylate – Rheology with simultaneous FTIR spectroscopy
- UV-induced curing reactions investigated by simultaneous rheometry FTIR measurements

### **Rheometry and Raman spectroscopy**

- Rheology-Raman spectroscopy: Tracking emulsion stability with the combination of a rheometer and a Raman spectrometer
- Rheology-Raman spectroscopy: Tracking polymer crystallization with the combination of a rheometer and a Raman spectrometer
- Tracking crystallization of EVA/acetaminophen mixtures with the combination of a rheometer and a Raman spectrometer
- Simultaneous rheology and Raman spectroscopy during the melting and recrystallization of polypropylene
- Investigating cocoa butter crystallization using simultaneous rheology and Raman spectroscopy (RheoRaman)

# Investigation of pharmaceutical hot-melts via simultaneous rheometry and polarization microscopy

Fritz Soergel,<sup>a</sup> Dirk Hauch,<sup>a</sup> Matthias Jährling,<sup>a</sup> Katharina Paulsen,<sup>a</sup> Astrid Weber-Kleemann,<sup>a</sup> Thorsten Cech,<sup>b</sup> Andreas Gryczke,<sup>b</sup> Stefan Schmölzer,<sup>c</sup> Damir Zecevic<sup>d</sup>

<sup>a</sup>Thermo Fisher Scientific, Karlsruhe, Germany | <sup>b</sup>BASF SE, Ludwigshafen, Germany | <sup>c</sup>NETZSCH-Gerätebau GmbH, Selb, Germany | <sup>d</sup>Boehringer-Ingelheim, Biberach, Germany

## Overview

**Purpose:** Provide on the one hand an efficient screening tool for hot-melt extrusion (HME) formulation development and make available on the other hand rheological parameters for process development and optimization, as well as for modeling calculations for compounding and extrusion.

**Methods:** Rheometry and polarization light microscopy up to 300 °C with well-defined heating and cooling rates, temperature profiles and shear rates as well as oscillatory testing.

**Results:** This combined method requires only a small sample volume and delivers efficiently significant and well-correlated rheological data and microscopic images, which allow to investigate formation and stability of solid solutions or crystalline dispersions. Moreover these results deliver at the same time meaningful parameters for extruder dimensioning and processability and for simulation calculations of the pharmaceutical HME process.

## Introduction

The simultaneous acquisition of rheological data and microscopic images is already an established research tool for a variety of applications in industries like e.g. food, petrochemicals and cosmetics. This combined method is applied to investigate processes like emulsification, coalescence, foaming and crystallization as well as for the determination of number, morphology and size distribution of crystals.<sup>1,2</sup>

## Formulation development

More recently, the pharmaceutical industry faces the challenge to find the right solubilizers and processing equipment/ parameters for newly developed Active Pharmaceutical Ingredients (APIs) to be able to process them and achieve high bioavailability, long term stability as well as good drug release characteristics. In order to produce a stable drug, the goal in R&D is to develop a formulation containing the API, suitable polymers or waxes (as solubilizers), plasticizers and processing additives, leading to a solid solution which does not show recrystallization.<sup>3,4</sup> With other APIs, the formulation of a crystalline dispersion may be the goal, because for those APIs crystal ripening may be less fatal regarding long term stability and drug release than a potential recrystallization of a solid dispersion.

Traditionally, different measurements have to be made parallel to each other, for example with a hot stage microscope with heating/cooling capability (to determine crystals and their melting and recrystallization behavior) or a Kofler Bench (metal plate with defined temperature gradient to determine softening and melting ranges in a subjective way). More comprehensive analytical methods are Differential Scanning Calorimetry (DSC; determines glass transition, melting/crystallization temperatures, melting/crystallization enthalpies) and Thermogravimetric Analysis (TGA; determines water content, thermal degradation).<sup>5</sup>

For hot melt extrusion, a screening tool is most beneficial which delivers consistent information about crystallinity in dependence of temperature and at the same time relevant parameters for processability — like softening, melting and degradation temperature and the information, how viscosity changes with temperature and with shear rate.

Process development/optimization and modeling  
 Simultaneous rheometry and polarization microscopy allows studying the melting behavior of crystals in the heating run, to investigate whether a recrystallization occurs in the cooling run and derive suitable processing parameters for compounding and extrusion.

Moreover, frequency sweeps measured at different temperatures can be superimposed to a so called “Master Curve“ utilizing time temperature superposition (TTS).<sup>6,7</sup> Master curves can be plotted for different relevant temperatures providing the respective relationship between viscosity curve and processing shear rates (Fig. 1) for process development/optimization and extruder dimensioning – depending on the temperature tolerance of the materials and the extruder characteristics like torque range and share rate range. Hence, the rheometer serves as a “Zero Level Extruder“ for pure components as well as for mixes with various components and concentrations of polymers, APIs, plasticizers and processing additives.<sup>8</sup>

Comparing the screening with a rheometer and with a small extruder, the rheometer on the one hand has a much higher throughput because of its much smaller sample volume (1 mL or less) and much shorter time for loading/

feeding and cleaning. On the other hand, the energy input in a rheometer in oscillatory testing is due to thermal energy while in an extruder the energy input is provided mainly mechanically by the screws.

Master curves are also capable of providing rheological input for process simulation calculations.<sup>5</sup> Process simulation can help identifying appropriate extruder setups as well as setting parameters and hence reduce material consumption and labor intensive development time (trial and error would be the alternative approach). Process simulation is a well established method in designing molds and flow channels, where it reduces development time as well as costs significantly.

Fig. 1 shows the viscosity curve of a technical polymer (LLDPE) at 220 °C as well as typical shear rate ranges for processing technologies (black) and a typical viscosity range for compounding and extrusion (grey). The viscosity data were acquired using oscillatory rheometry (blue; Thermo Scientific™ HAAKE™ MARS™) and extrusion capillary rheometry with a torque rheometer (Thermo Scientific™ HAAKE™ PolyLab™) equipped with a slit capillary die (red) or a rod capillary die (green). According to the empirical

Cox-Merz Relation, the oscillatory complex dynamic viscosity as a function of angular frequency (blue) and the complex viscosity as a function of shear rate (red and green) can be superimposed for unfilled polymer melts and polymer solutions, as shown in Fig. 1. This is the reason why data measured in oscillation can be used to predict the processability in compounding and extrusion.<sup>7</sup>

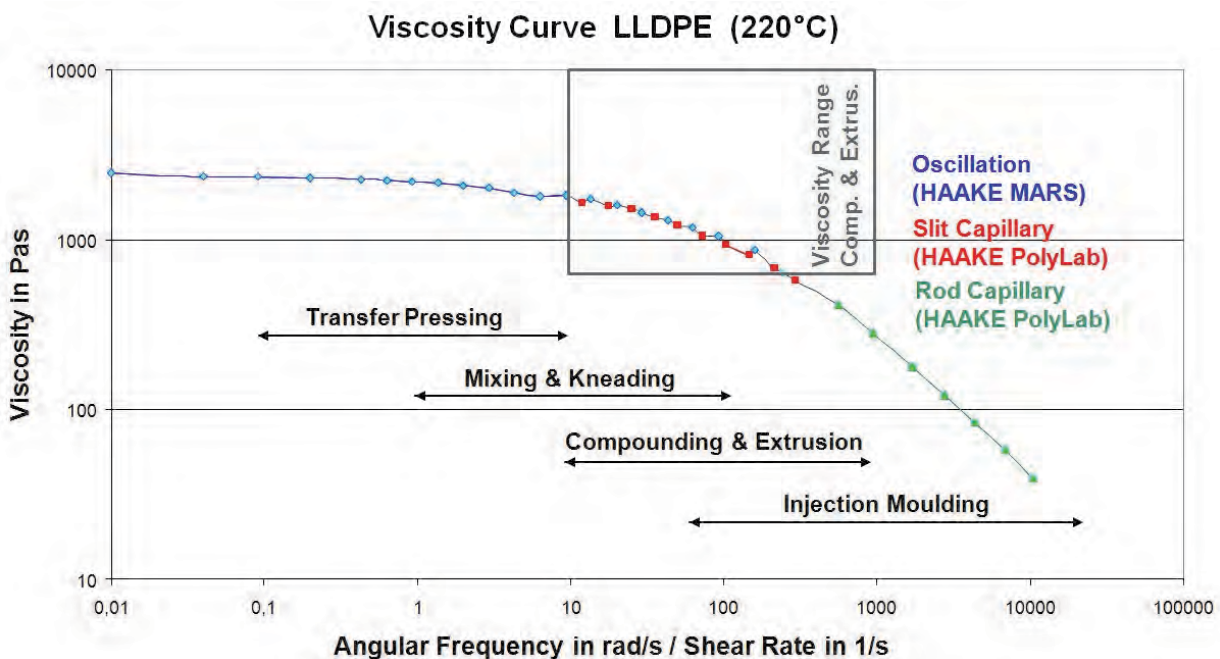


Fig. 1: Viscosity curve of LLDPE and typical shear rate ranges in rheometry as well as in polymer processing.

## Materials

An essential requirement for HME investigations is that all kind of samples from all processing steps, i.e. powder, extrudate and injection molded samples, can be characterized — pure components and mixes as well.<sup>5</sup>

For our investigations, we selected as model systems Soluplus® (BASF, approved for pharmaceutical applications,<sup>3</sup> Fig. 2) as polymer and Ibuprofen (BASF, ACROS) as well as Theophylline (BASF) as APIs.



Fig. 2: BASF Soluplus® powder.<sup>3</sup>

## Powder (ground)

With a spatula, a disc-shaped powder layer was formed (diameter 35 mm, thickness approx. 2 mm). Using the normal force control capability of the HAAKE MARS rheometer, a normal force of 30 N to 40 N was applied with the plate/plate measuring geometry, in order to interlock the particles, so that an amplitude sweep and a frequency sweep with the powder could be recorded at sample loading temperature. The amplitude sweep delivered the Linear Viscoelastic Range (LVR) with the powder and allowed to determine a suitable deformation amplitude range for the subsequent measurements — with too low oscillation amplitude the signal-to-noise ratio would have been insufficient, with too large amplitude the powder would have been conveyed out the sample gap.

The heating ramp revealed the softening and melting behavior of the powder sample (for example: Fig. 9). After the sample was molten, the sample gap was under filled and filling needed to be optimized by closing the gap further, then the heating run could be finished, followed by a cooling run (for example: Fig. 11).

If heating curves are requested or the melting behavior of crystals needs to be investigated (Figs. 9, 10), extruded as well as injection molded samples can be ground and then treated as described above.

## Extrudate (pellets, strand)

While powder can be loaded and measured at ambient temperature, extrudate sample loading requires melting of the extrudate pieces in order to obtain a proper mechanical coupling between measuring geometry and sample as well as proper filling of the measuring gap. Pellets or strand pieces were placed on the lower part of a plate/plate measuring geometry at a temperature above the sample's melting temperature (Fig. 3). Then the upper geometry was lowered step by step while the sample was melting. Finally, the sample rim was trimmed (cylinder-shaped) with a trimming tool.<sup>9</sup> Afterwards the sample gap was closed by 5% to 10% in order to obtain ideal gap filling (slightly barrel-shaped). Then amplitude and frequency sweeps of the melt and a cooling ramp were measured.



Fig. 3: Extrudate pieces placed on the lower plate of the measuring geometry for melting and subsequent loading and trimming.

## Cast (injection molded discs and bars)

Compared to extrudate pieces, injection molded discs can be loaded quicker and easier into a plate/plate measuring geometry at elevated temperatures and the completeness and reproducibility of gap filling (and therefore of the rheological data) is much better.

Injection molded solid bars can be measured in the glassy and rubbery state with DMTA solid sample clamps<sup>10,11</sup> in the CTC oven (Fig. 4) of the Thermo Scientific HAAKE MARS rheometer to investigate e.g. the impact of ingredients and processing parameters (like screw configuration, filling degree, residence time, temperature and shear rate) on the glass transition characteristics.<sup>13</sup>

Advantages of the self-centering and self-tightening spring-loaded DMTA solid sample clamps are faster loading (neither thickness measurement nor spacer adaption required), excellent reproducibility (self-centering) and no need to reopen the oven at lowest temperature for retightening of the solid sample clamps with the related issues of humidity precipitation and ice formation on sample clamp and measuring shaft (self-tightening).

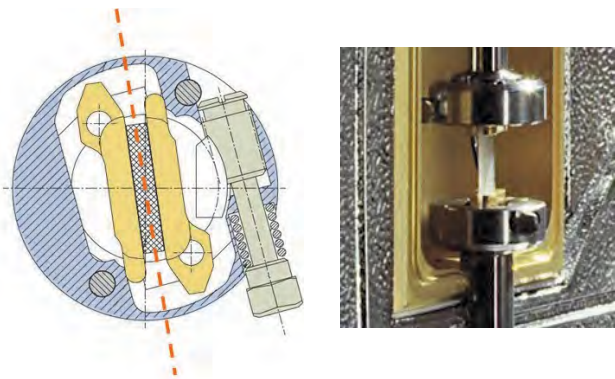


Fig. 4: Self-centering and self-tightening spring-loaded DMTA solid sample clamps (drawing left) in a CTC oven and with an injection molded bar sample (right).

## Methods

With the Thermo Scientific Material Characterization portfolio, a HME workflow can be easily investigated. The rheometer serves as a screening tool and as a “zero level extruder” and provides information regarding processing parameters and extruder dimensioning. For easy scale up, a family of 11 mm, 16 mm and 24 mm parallel twin screw extruders is available all of them having the same set of dimensionless quantities for smart scalability<sup>5,8</sup>. Differential Scanning Calorimeters (DSC) and Thermo Gravimetric Analyzers (TGA) are part of the portfolio of our cooperation partner NETZSCH Analyzing & Testing.

The powder samples were fed into the Thermo Scientific™ HAAKE™ MiniLab for compounding and (after switchover via the pneumatically actuated bypass valve) for extrusion of a strand. The Thermo Scientific™ HAAKE™ MiniLab can be used with counter-rotating conical twin screws for conveying or with corotating conical twin screws for mixing — deployed here. A part of the back flow channel is a (relatively wide) slit capillary die with two pressure sensors (Fig. 5), facilitating viscosity measurements in the shear rate range from 1 to 100 1/s.

The extruded sample material from the HAAKE MiniLab was directly transferred into the temperature-controlled sample container of the Thermo Scientific™ HAAKE™ MiniJet mini injection molding machine, which was used for the injection molding of sample discs and DMTA sample bars (Fig. 6).

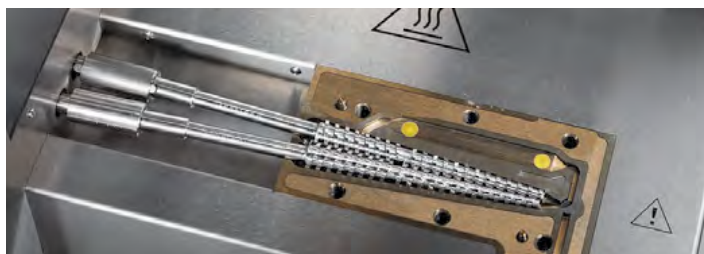


Fig. 5: HAAKE MiniLab can be used with counter-rotating or corotating conical twin screws (center), has a bypass valve (right), a back flow channel with a slit capillary with two pressure sensors for viscosity measurement (top) and an extrusion channel (bottom right).



Fig. 6: HAAKE MiniJet molds with injection molded samples of different shape and size.

For rheometry, the HAAKE MARS rheometer was used with a temperature controlled polarization microscope (Thermo Scientific™ HAAKE RheoScope™ module with electrical hood™ EL-H, cold light source, lens 5 x or 20 x) and a 20 mm plate rotor or a 35 mm plate rotor with polished surface for enhanced quality of the microscopic images. The resolution with the 20 x lens was 1 μm, the temperature range up to 300 °C. For powerful and well-controlled counter-cooling, a refrigerated circulator was used — the bath temperature adjusted 10 K to 20 K below the minimum measuring temperature. The bath fluid’s flow rate was controlled via continuously adjustable valves in the HAAKE MARS rheometer. At subambient temperatures, the lens was kept clear by flushing it with a small flow rate of dry purge gas.

Two polarization filters can be moved into the ingoing and outgoing optical paths (Fig. 7) and one of the both filters can be rotated to cross the polarization filters for contrast enhancement and for discrimination of crystalline or birefringent structures.

Polarization filter (on/off, angle adjustment), lens (radial and focus adjustment) as well as camera control (contrast, brightness, gamma, (auto)integration time) are all set and controlled via the Thermo Scientific™ HAAKE™ RheoWin™ software, which allows furthermore to save and load different sets of settings also within a measuring job: E.g. at first images of the melt without polarization filters can be recorded at elevated temperatures to discriminate different kind of particles and then, during the cooling run, images with crossed polarization filters to capture crystal growth. Changing the lens is also possible while the sample is in place.

The glass transition temperatures were determined by means of Differential Scanning Calorimetry (DSC). For the presented measurements, the NETZSCH DSC 204 F1 Phoenix® was used with autosampler and with Aluminum

crucibles with pierced lids. With this method, the powder samples could be easily prepared and investigated as well as the injection molded samples.

Fig. 8 shows a cross section through the measuring cell. The heat flux sensor is incorporated in the cylindrical silver furnace. With its homogeneously heated disc-sensor system, this set-up provides stable and reproducible baselines. Different cooling equipment is available so that a temperature range from  $-180\text{ }^{\circ}\text{C}$  to  $700\text{ }^{\circ}\text{C}$  can be covered.

## Results

### Ibuprofen – enantiomer and racemate

Pure Ibuprofen powder was loaded at room temperature into a 35 mm plate/plate measuring geometry and pressed with a normal force of several 10 N. After an amplitude sweep, a heating run was measured with  $1\text{ K/min}$ . The thermal expansion of the measuring set-up was

compensated automatically by using the ThermoGap functionality provided by the HAAKE RheoWin software.

When Ibuprofen melts, its complex dynamic viscosity  $|\eta^*|$  and its storage modulus  $G'$  change both dramatically over approx. 7 orders of magnitude – which has of course a major impact on the processability (Fig. 9). The melting temperature is strongly affected by the chirality of the Ibuprofen. The cross-over temperature, where the storage modulus  $G'$  equals the loss modulus  $G''$  and the phase angle  $\delta$  equals  $45^{\circ}$  was evaluated. The racemate (BASF) melts at  $77\text{ }^{\circ}\text{C}$  whereas the enantiomer (ACROS) melts at  $52\text{ }^{\circ}\text{C}$ . The racemate is a mixture of two types of enantiomers and reveals a change in the slope of the normal force vs. temperature curve  $F_n(T)$  at that temperature at which the first enantiomer's melting is completed. Two tangents were fitted to the two slope regimes and the intersection point of the tangent was determined ( $57\text{ }^{\circ}\text{C}$ ).

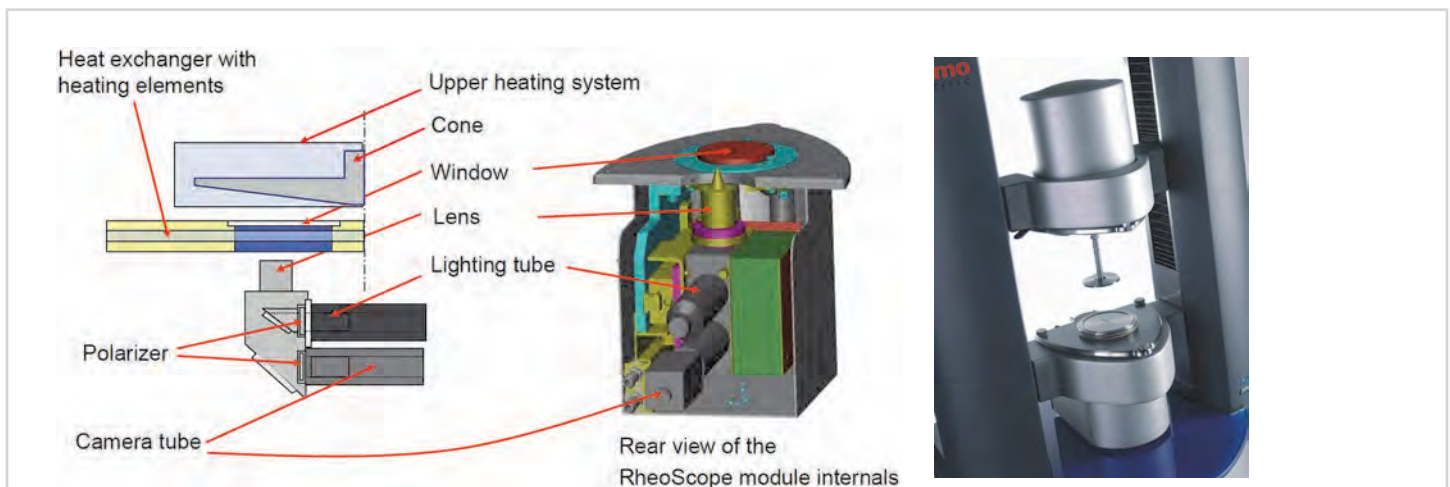


Fig. 7: HAAKE RheoScope module: Schematic drawing (left: side view, center: rear view) and mounted in the HAAKE MARS rheometer (right).

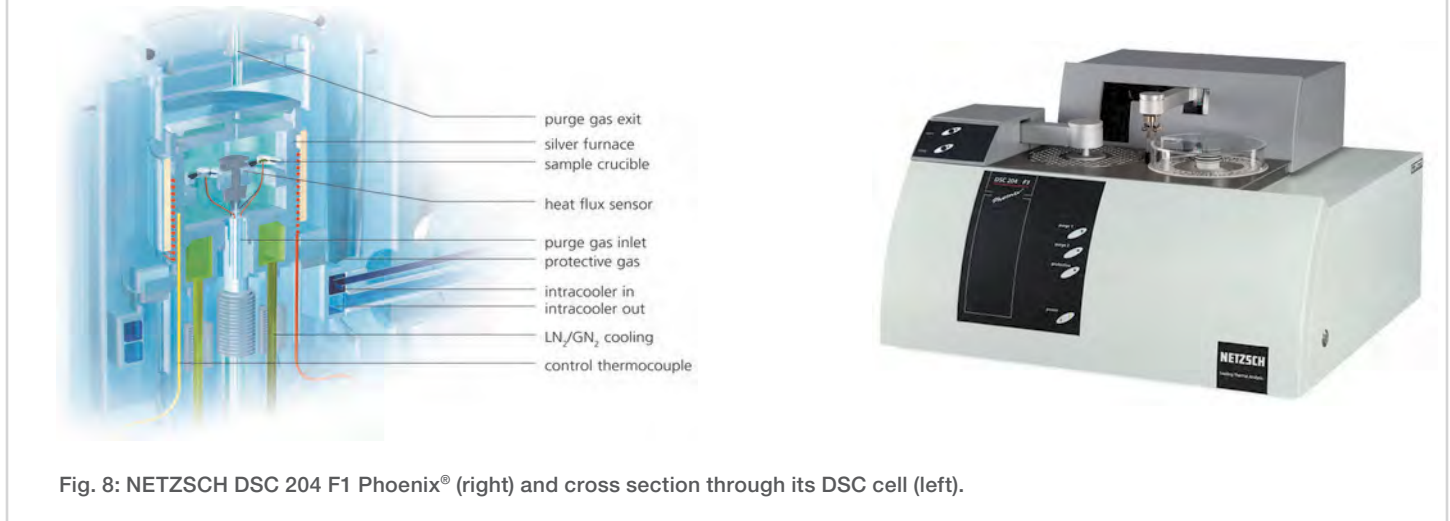


Fig. 8: NETZSCH DSC 204 F1 Phoenix® (right) and cross section through its DSC cell (left).

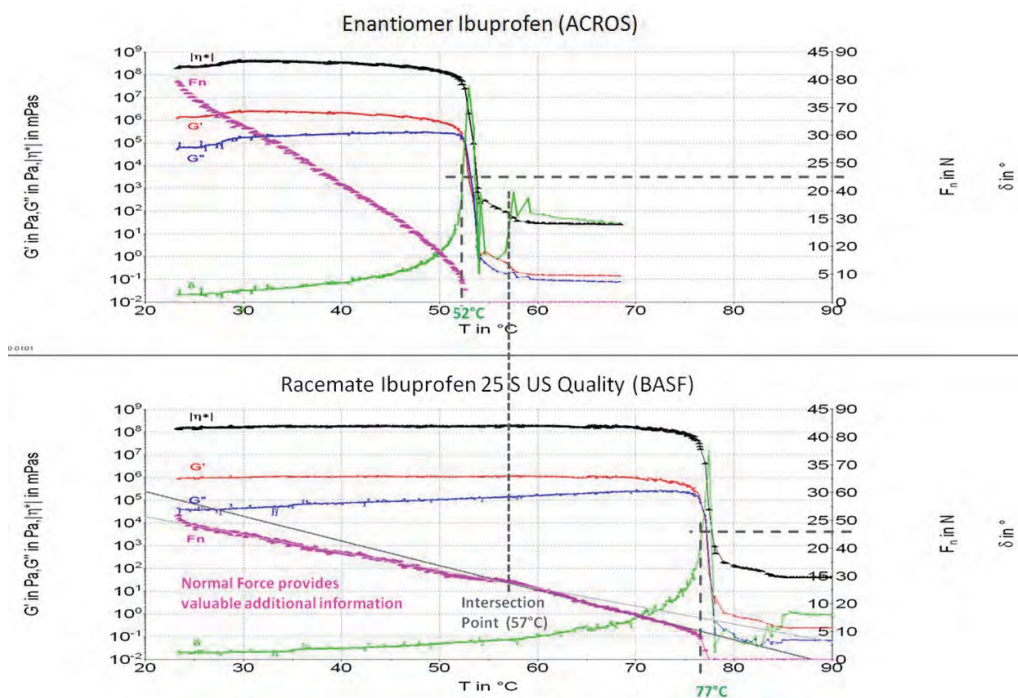


Fig. 9: Heating runs (1 K/min) with Ibuprofen powder (top: enantiomer, bottom: racemate), chirality indicated symbolically top left (measuring amplitude: 0.1% with powder, first 10% then 30% with fluid, measuring mode: CD-AS<sup>14</sup>).

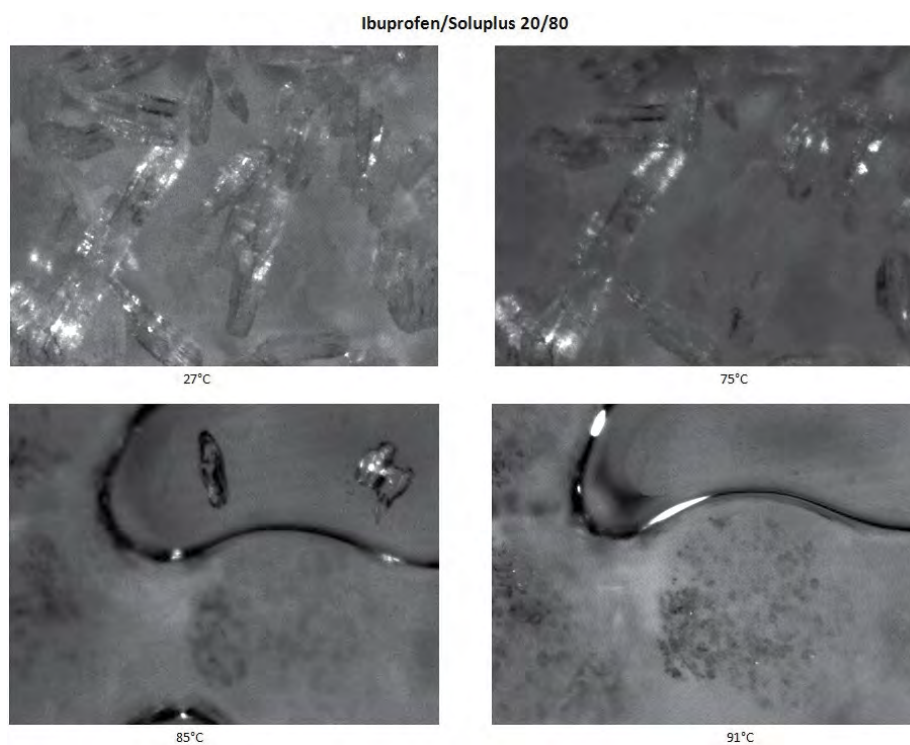


Fig. 10: Powder mix with 20% Ibuprofen and 80% Soluplus® at 27 °C (top left) and gradual melting of the API shown in images taken at 75 °C, 85 °C and 91 °C (lens 20 x).

### Ibuprofen in Soluplus®

Polarization microscope images of crystalline Ibuprofen powder (racemate) mixed with Soluplus® powder are shown in Fig. 10. The images were obtained with crossed polarization filters revealing size, morphology and spatial distribution of crystals and their melting with increasing temperature. For the analysis of particle size or particle size distribution, an image analysis software (e.g. SPIP by Image Metrology<sup>12</sup>) can be employed.

In a subsequent cooling run, no recrystallization of the Ibuprofen occurred. Thereafter, the samples would usually be subjected to long-term stability testing according to currently valid ICH guidelines. Typical parameters for such tests are 25 °C and 60% relative humidity (RH) for standard stability testing and 40 °C and 75% RH for accelerated aging.<sup>5</sup> Evaluation is made typically (e.g. after 1, 2, 4 and 8 weeks and 3, 6, 12 and 24 months).

## Soluplus® — pure and with 10% or 30% Theophylline

Theophylline has a very high melting point (270 °C), which allows studying the impact of this API on the glass transition of the polymer Soluplus®. Fig. 11 shows cooling ramp results with 3 powder samples, which had been heated up to 140 °C for sample loading and trimming in a plate/plate measuring geometry. From these 3 powder samples, additionally, injection molded samples (potential residual strains) were made with the HAAKE MiniLab and HAAKE MiniJet and measured with DMTA solid sample clamps in the CTC oven with a heating ramp, see Fig. 12.

In both measurements, the pure Soluplus® sample (black) shows a higher glass transition temperature than the samples containing 10% (red) or 30% (blue) Theophylline. Theophylline has obviously a plasticizer effect, which shifts the glass transition of Soluplus® to lower temperatures. Interestingly, the 10% sample shows this effect to a higher extent than the 30% sample. DSC measurements confirm these findings (Figs. 13, 14).

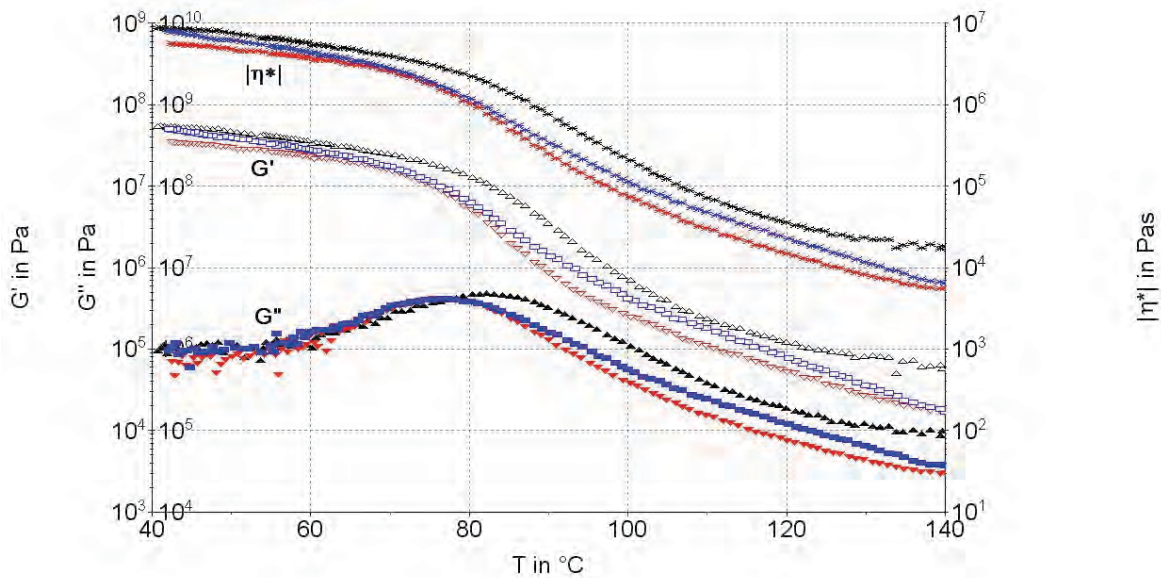


Fig. 11: A cooling run (-5 K/min) with 3 powder samples molten at 140 °C with different Theophylline concentrations (0% black, 10% red, 30% blue) in Soluplus® measured in plate/plate measuring geometry (measuring amplitude: 0.01 %, measuring mode: CD-AS<sup>14</sup>).

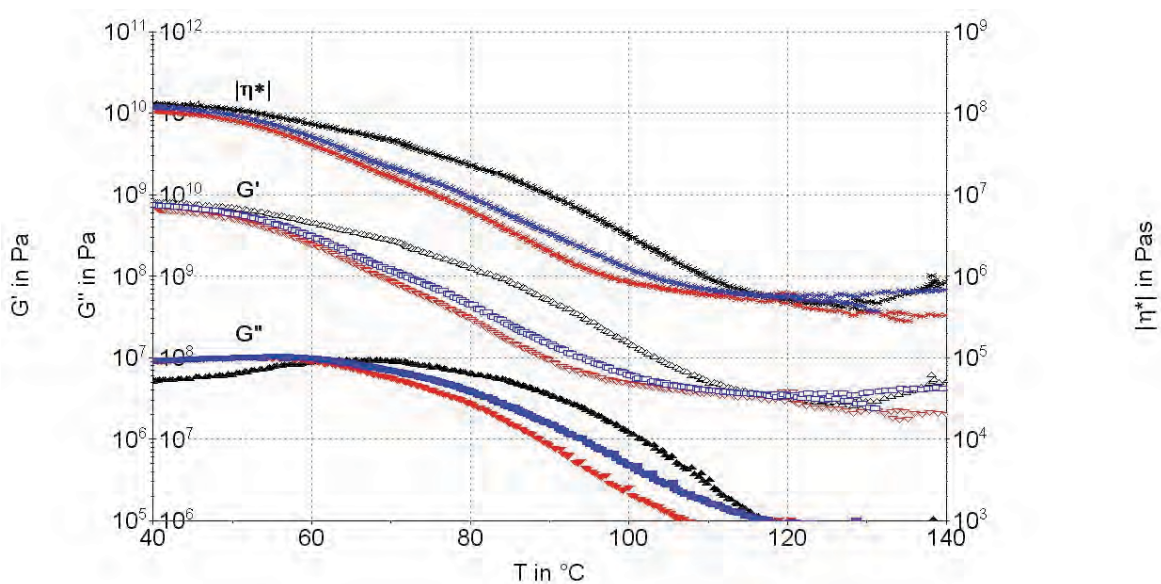


Fig. 12: D heating run (5 K/min) with 3 injection molded rectangular bars with different Theophylline concentrations (0% black, 10% red, 30% blue) in Soluplus® measured with DMTA clamps (measuring amplitude: 0.01 %, measuring mode: CD-AS<sup>14</sup>).

## Discussion

### Absolute values of the storage modulus

The storage modulus  $G'$  of an unfilled and non-crystalline polymer is typically slightly above 109 Pa in the glassy state and 106 Pa in the rubbery state. Filler particles or crystals increase the  $G'$  value in the rubbery state considerably. To increase  $G'$  in the glassy state slight, high-impact filler particles or fibers (e.g. nanotubes) were required.

For the measurements with the DMTA clamps, torsional deformation is applied. As long as small amplitudes are used, a pure shear deformation of the sample bar is generated (only large amplitudes would lead to a superposition of shear deformation and of elongational deformation). The DMTA measurements with injection molded solid bars (shown in Fig. 12) are really consistent. The glassy state plateau would be fully reached at temperatures lower than the measured ones.

Cooling runs with molten powder or extrudate particles in a plate/plate measuring geometry deliver on the one hand correct temperatures for the maxima in  $G''$  (for the regarding cooling rate) but do on the other hand usually not reach the correct value for  $G'$  in the glassy state with 20 mm diameter (or bigger) because the measured deformation is then partly related to the glassy sample and partly to the torsional deformation of the measuring geometry (Fig. 11). Therefore, using DTMA solid sample clamps is mandatory for a correct determination of  $G'$  in the glassy state.

Powder samples, however, may have further effects on the  $G'$  data: Fig. 9 shows that there is no full coupling between the measuring geometry and the powder sample at the beginning of the heating run (up to 29 °C). Above 29 °C, the temperature-induced softening brings about full coupling. But still, the powder in the measuring gap has plenty of hollows leading to considerably lower  $G'$  values. The hollows disappear when the powder sample is melting – which of course leads to a significant under filling of the measuring geometry and the measuring gap needs to be closed manually in order to obtain proper filling and correct  $G'$  data with the molten sample.

### Comparison of DTMA and DSC results

The glass transition, i.e. the loss of molecular mobility during cooling, makes itself apparent in dynamic mechanical properties as well as in specific volume, enthalpy, entropy, specific heat, refractive index etc. The glass transition data obtained with different methods are interlinked over the activation diagram<sup>7</sup>.

In Fig. 13, the DSC curves for the second heating run on the powder samples with different concentrations of Theophylline in Soluplus® are shown: The samples were heated up with a constant heating rate of 10 K/min under nitrogen atmosphere. As the samples lost moisture (which was verified with TGA measurements) always the curve of the second heating run was evaluated.

The glass transition can be seen very clearly in these measurements as a change in the specific heat capacity, i.e. as a step in the DSC heat flow curve. Pure Soluplus® (black) shows the highest  $T_g$  and the sample with 10 % Theophylline (red) the lowest  $T_g$ . It is also evident from the results, that a further increase of the Theophylline content (30%, blue) does not lead to a lower  $T_g$  than with the 10% sample.

The results for the injection molded samples are shown in Fig. 14. Here the same trend in the shift of  $T_g$  with the Theophylline concentration could be found. Furthermore, it is remarkable that for all three molded samples,  $T_g$  is shifted to lower temperatures compared to the powder samples. This effect is most likely due to the processing of the material in HAAKE MiniLab and MiniJet altering the thermal history of the samples – which can be detected by means of Thermal Analysis.

The evaluation of the DSC “mid step height“ (second heating run; no residual strains, Figs. 13, 14) and the maximum in the DTMA loss modulus curves  $G''(T)$  (measured with a frequency of 1 Hz, Figs. 11, 12) are delivering similar results for the glass transition temperature. Strictly speaking, an extrapolation from higher heating/cooling rates (DSC: 50, 20, 10 K/min, DTMA: 5, 2, 1 K/min) to 0 K/min would deliver the correct results – only then the hysteresis between heating and cooling runs would disappear (if then still a hysteresis would appear, it would be related e.g. to undercooling).

However, there are several differences between the DSC and DMTA method, which need to be taken into consideration – also for hot melt characterization. DSC is a static method while DMTA is a dynamic method. A risk is that without mechanical deformation, DSC samples may turn into an undercooled melt due to a lack of crystallization seeds.

The glass transition temperature can be detected with both methods very precisely. The impact of side chains and lower temperature glass transitions as well as anisotropy (e.g. direction of production or fiber direction in reinforced materials) can usually not be detected with DSC, but DMTA has a high sensitivity for these effects.

Advantages of DSC measurements are that they only require a small sample quantity, can be run in series with an autosampler, with high heating and cooling rates and are therefore used as an essential screening tool for HME formulation development, providing glass transition, melting, crystallization temperatures as well as melting and crystallization enthalpies.

Rheometry/DMTA measurements, on the other side, are closer to what happens in an extruder (Fig. 1). In addition to temperature-dependent measurements (glass transition, softening, melting and crystallization temperature), they can provide amplitude- and time-dependent as well as frequency- dependent measurements (Figs. 1, 11, 12), which allow to study e.g. the impact of plasticizers and provide data for determination of molecular weight MW and molecular weight distribution, processability prediction and modeling calculations<sup>7</sup>.

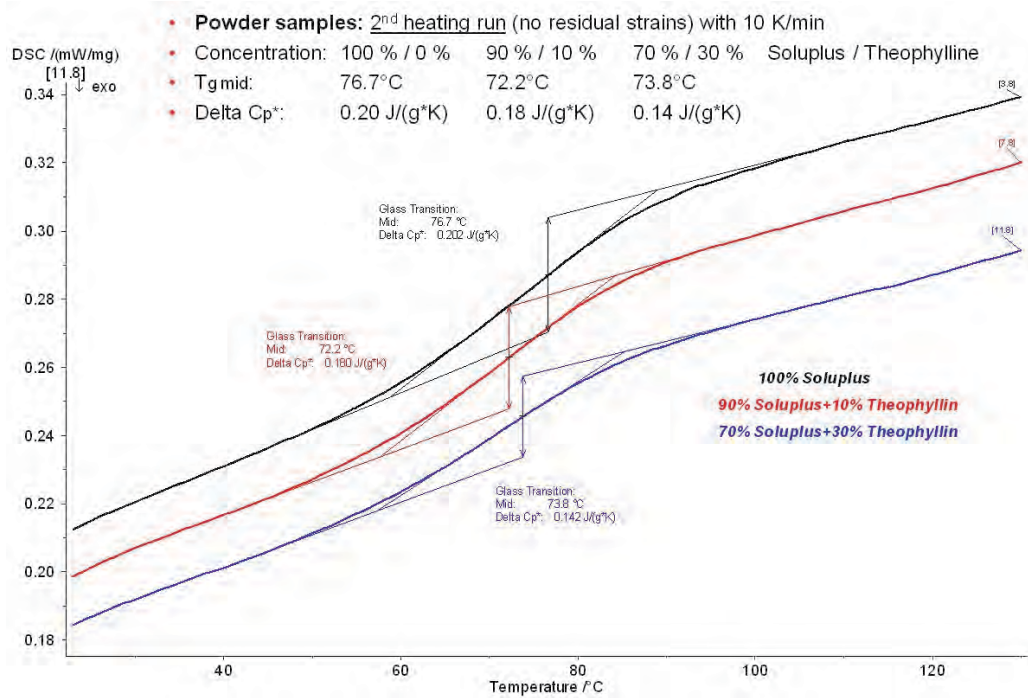


Fig. 13: DSC measurements — second heating run (10 K/min) with 3 powder samples with different Theophylline concentrations (0% black, 10% red, 30% blue) in Soluplus®.

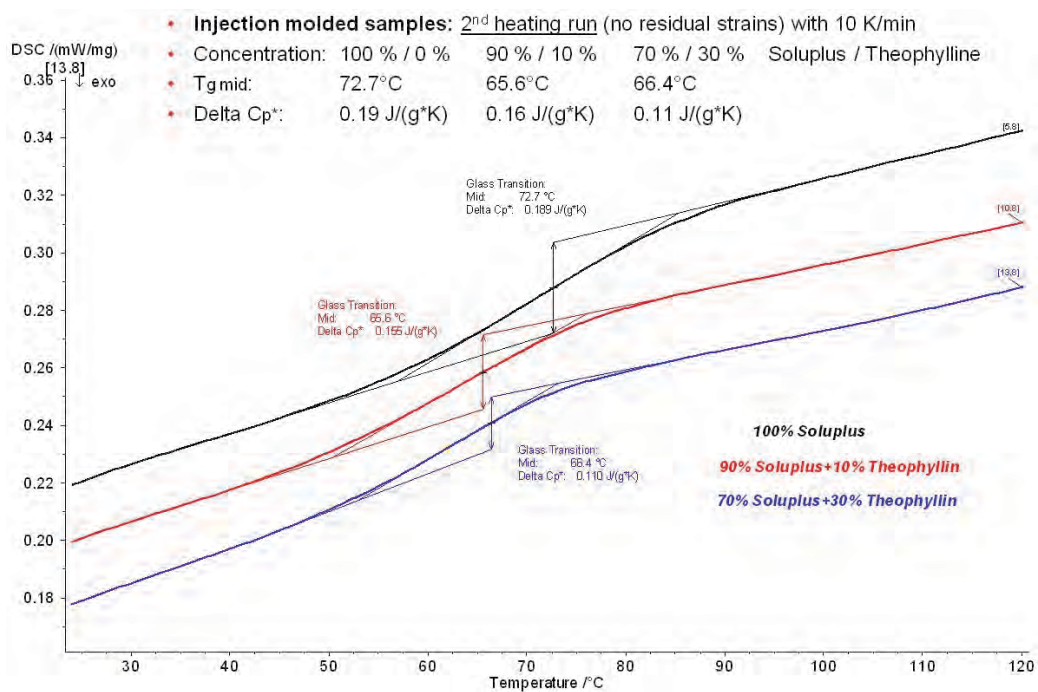


Fig. 14: EDSC measurements — second heating run (10 K/min) with 3 injection molded samples with different Theophylline concentrations (0% black, 10% red, 30% blue) in Soluplus®.

## Conclusion

The HAAKE MARS equipped with the HAAKE RheoScope module delivers a consistent set of simultaneously acquired rheological data and polarization microscopy images for purposeful hot melt formulation development and process development/optimization as well as for modeling calculation input. This combined method allows investigating pure polymers, pure APIs and mixtures of those – also with plasticizers and additives and reveals whether an amorphous solid dispersion or a crystalline solid dispersion is obtained during heating and whether it is stable during cooling or storage.

Rheometry married together with microscopy, providing well defined heating and cooling rates. is a highly efficient screening tool delivering parameters which are traditionally collected with several methods parallel to each other using different equipment (examples in brackets): Crystal concentration, morphology and distribution and their melting behavior (hot stage microscope), temperatures of softening, melting or thermal decomposition (Kofler Bench, DSC or TGA) as well as information about the glass transition (DSC). Compared to information acquired with different equipment, simultaneously collected information requires less sample, has a better correlation and higher reproducibility and is more efficient, consuming less lab space and is more cost-conscious. For a fast screening of a large number of formulations, however, always a DSC with autosampler will be employed.

Rheometry is a dynamic mechanical method and therefore close to compounding and extrusion and delivers with its temperature curves and master curves on the one hand processing parameters (softening, melting and degradation temperature as well as angular frequency/shear rate range) and on the other hand input, which is required for extruder dimensioning and modeling calculations. Therefore, rheometry serves as a “zero level extruder“. Compared to a small extruder regarding sample volume and time required for feeding, compounding and extrusion as well as cleaning, the rheometer allows a much faster screening of different combinations and concentrations of polymers,

APIs, plasticizers and additives for process development. With the most promising formulations, compounding and extrusion is then tested and optimized with a small extruder, because the energy input in a rheometer in oscillatory testing is due to thermal energy whereas in an extruder the energy input is mainly due to the mechanical energy provided by the screws.

With a family of easy scalable 11 mm, 16 mm and 24 mm twin-screw extruders (with the same set of dimensionless quantities), the subsequent scale-up can be achieved most time- and cost-efficient and reduces the time to market considerably.

## References

1. Oldörp K. What happens when rheological properties change? Looking into rheological properties with simultaneous collection of microscopic images. Thermo Scientific Application Note V-228 (2009)
2. Oldörp K. Waxing of Crude Oil – An Easy Approach with Rheooptical Methods. Thermo Scientific Application Note V-241 (2009)
3. Kolter K., Karl M., Gryczke A. Hot-Melt Extrusion with BASF Pharma Polymers – Extrusion Compendium. 2nd revised and extended edition. BASF SE, Ludwigshafen, Germany (2012)
4. Gryczke A., Ziegler I. Hot-Melt Extrusion Master Class. Seminar Materials, APV – International Association for Pharmaceutical Technology, Mainz, Germany (October 2011)
5. Douroumis D. (ed.) Hot-melt extrusion: Pharmaceutical applications. Wiley (2012)
6. Fischer A. Time-Temperature-Superposition (TTS). Thermo Scientific Application Note V-226 (2007)
7. Wraha C. Introduction to Polymer Physics. LANXESS Books (2009)
8. Paulsen K. Scale-up approach in HME. Proceedings of the APS meeting “Amorphous IV: Hot-melt extrusion and powder technology in pharmaceutical industry“. Greenwich 12th-13th June 2012
9. Küchenmeister C., Oldörp K. Trimming tool to remove overfilling in a plate/plate and cone/plate measuring geometry. Thermo Scientific Product Note P-003 (2009)
10. Oldörp K., Nijman J., Küchenmeister C. Measurements on selected (semi-)solids in a wide temperature range using new solid clamps. Thermo Scientific Application Note V-220 (2006)
11. de Jong F., Oldörp K. Dynamic Mechanical Thermal Analysis (DMTA) on Polymer Composites with the HAAKE MARS Rheometer. Thermo Scientific Application Note V-241 (2009)
12. Küchenmeister C., Sierró P., Soergel F. SPIP software for analysis of RheoScope images. Thermo Scientific Product Note P-009 (2009)
13. Eidam D., Hauch D., Jakob B. Influence of additives on processability and rheological properties of pharma polymers. Thermo Scientific Application Note LR-64 (2008)
14. Meyer F., Schulz U., Soergel F. Oscillatory Measurements in CS-, CD- or CD-AutoStrain-Mode. Thermo Scientific Application Note V-245 (in prep.)

## Acknowledgements

We would like to thank Dr. Cornelia Küchenmeister-Lehrheuer and Dr. Jan Philip Plog (both Thermo Fisher Scientific, Karlsruhe, Germany) for carefully reviewing this application note, for their valuable input and for presenting a part of it at the International Congress on Rheology 2012 in Lisbon Portugal.

Find out more at [thermofisher.com/rheometers](http://thermofisher.com/rheometers) and [thermofisher.com/extruders](http://thermofisher.com/extruders)

**ThermoFisher**  
SCIENTIFIC

# Image acquisition with the HAAKE RheoScope module at high shear rates using a stroboscope light source and contrast enhancing illumination

Fritz Soergel, Fabian Meyer, Philippe Sierro and Cornelia Küchenmeister-Lehrheuer  
Thermo Fisher Scientific, Karlsruhe, Germany

## Overview

**Purpose:** During processing and application, shear rates in the order of 10,000 to 100,000 s<sup>-1</sup> may occur over shorter or longer times, which can lead e.g. to breaking or coalescence of emulsions or other unwanted effects, causing a change in morphology or particle size distribution.

**Methods:** For characterization of the emulsification process and for investigation and optimization of the further processing and/or application of emulsions, simultaneous rheometry and microscopy is a really powerful tool.

**Results:** Sharp microscopic images can be achieved at shear rates up to 50,000 s<sup>-1</sup> using a stroboscope instead of a cold light source. For emulsions with low optical contrast, the quality of the images can be improved significantly by adding a half circle diaphragm in the lighting tube.

## Introduction

Emulsions play an important role in food, pharmaceutical, cosmetics and many other areas. During the emulsification process it is desired to achieve a defined droplet size distribution. In the further processing of emulsions as well as in their application, the material is subject to mechanical shear stresses, which can lead to breaking,<sup>1</sup> coalescence (Fig. 2) or other unwanted effects causing a change in morphology or particle size distribution.<sup>2,3</sup> Furthermore, the stability achieved by proper formulation and processing, can be negatively affected by inappropriate storage conditions.

Using a technique that, on the one hand, simulates and, on the other hand, measures the effects of all these influences, enables designers and manufactures to optimize formulations and processing as well as product performance.

For a deeper understanding of structure-properties relationships, usually more than one analytical technique is required. However, when samples are tested on two separate analytical instruments, the comparability and reproducibility of the results have certain limitations. Only when exactly the same material is subject to a simultaneous investigation, these limitations can be overcome.

Rheometry delivers an integral mechanical response of the investigated sample (bulk properties) under stress or deformation. The mechanical properties, however, are directly related to the molecular and microscopic structure as well as its changes with time, temperature and mechanical impacts.<sup>1, 4-6</sup>

Combining traditional rheometry with other analytical techniques allows for a comprehensive investigation and provides a more complete picture of the sample characteristics. The comparability of all data sets is guaranteed and reproducibility is improved. Efficiency is higher, while sample consumption and lab space requirements are minimized. Finding the right complementary technique is a key factor for maximizing the information gained. Optical as well as spectroscopic

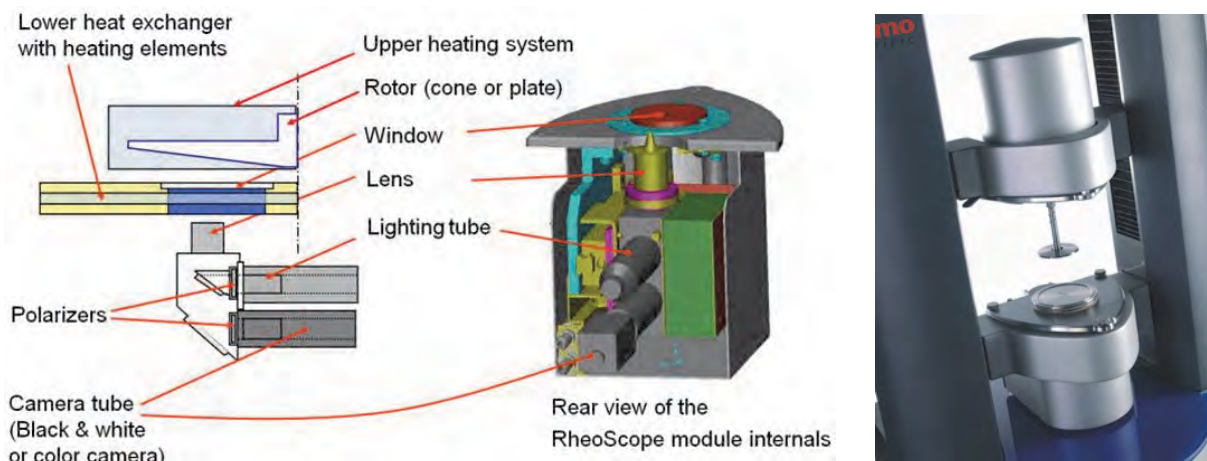


Fig. 1: HAAKE RheoScope module: Schematic drawing (left: side view, center: rear view) and mounted in the HAAKE MARS rheometer (right).

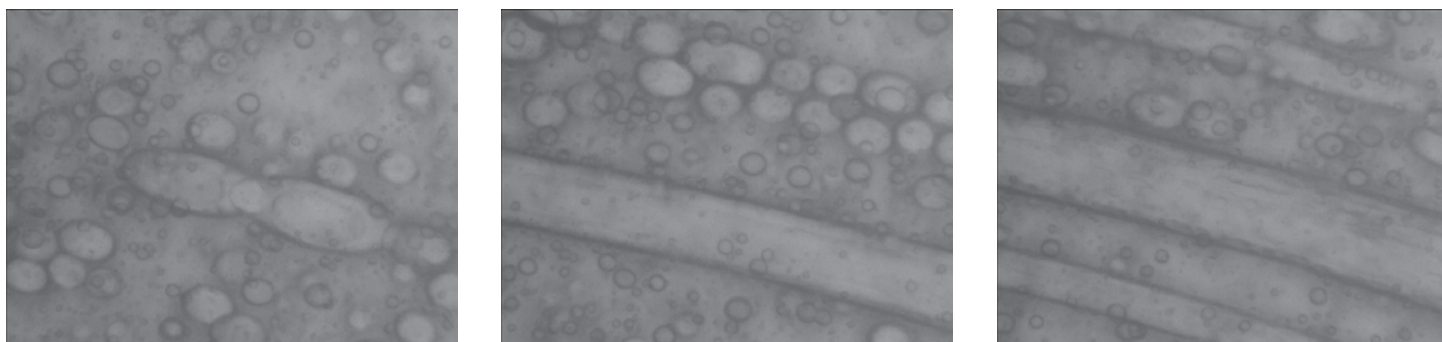


Fig. 2: Coalescence: at  $500 \text{ s}^{-1}$  applied for 0.3 s (left) and for 5.4 s (center) as well as at  $1000 \text{ s}^{-1}$  applied for 4.8 s (right).

methods provide structural information beyond the dynamic-mechanical response and are therefore predestinated for simultaneous application with rheometry.

**Simultaneous rheometry and light microscopy** The combination of rheometry with light microscopy (with or without polarization filters) allows, on the one hand, to study the change of a material's structure and properties with shear rate in rotational measurements. The recorded microscopic images reveal the induced structural changes like orientation, deformation, coalescence, aggregation or disaggregation. On the other hand, stress/strain or temperature dependent changes, like e.g. crystallization, can be investigated with non-destructive oscillatory measurements.<sup>4-6</sup>

The Thermo Scientific™ HAAKE RheoScope™ module (Fig. 1) is a compact accessory for the Thermo Scientific™ HAAKE™ MARS™ rheometer (Modular Advanced Rheometer System), integrating an optical microscope, a video camera and a temperature control unit (-5 °C to 300 °C). The typical resolution limit of a light microscope (1  $\mu\text{m}$ ) is already reached when the HAAKE RheoScope module is equipped with a x 20 lens – alternatively x 5 x 10 or x 50 lenses can be mounted. Plate/plate and plate/cone measuring geometries with a diameter up to 60 mm

can be used. For improved image quality with transparent samples, rotors with polished surface are available.

The complete control of the optical components is fully integrated in the measuring software, including radial positioning of the lens and focus adjustment. Both polarization filters can be moved into and removed out of the optical paths as shown in Fig. 1. Additionally, the polarization can be crossed by angular adjustment. Contrast, brightness, gamma value and (auto) exposure time of the camera can be set. Complete sets of all these parameters can be saved and loaded – e.g. for using different parameter sets for different states of a sample within one measuring job. Rheological data and microscopic images are one-to-one correlated and can be viewed during measurement and analysis.

Coalescence can occur in a salad dressing even at lower shear rates and within a short time. Fig. 2 depicts such an experiment: First a constant shear rate of  $500 \text{ s}^{-1}$  was applied in CR mode (controlled rate), followed by a shear stress of 0 Pa for 10 s in CS mode (controlled stress), then twice the initial shear rate was applied ( $1000 \text{ s}^{-1}$  in CR mode). The HAAKE RheoScope module was equipped with a x 20 lens (images size 640 x 480  $\mu\text{m}$ ). A C60/1° Ti rotor with polished surface was used.

## High shear imaging

Particle and droplet sizes as well as their size distributions can be determined, even at (very) high shear rates using a stroboscope (Fig. 3) instead of a cold light source, connected to the same light guide — swapping requires no tools and takes only a few seconds. Sharp microscopic images can be achieved up to  $50,000\text{ s}^{-1}$  with the stroboscope, while with a cold light source (depending on the individual sample) images up to a shear rate of  $2000\text{ s}^{-1}$  can be taken. This means, that the use of a stroboscope with the HAAKE RheoScope module extends the measuring range by a factor of 25 and more.<sup>7</sup>

Thanks to the stroboscope, e.g. the behavior of paints and inks during the coating process or the coalescence of emulsion droplets under (very) high shear rates can be investigated with the HAAKE RheoScope module. Shear-induced orientation and deformation in a sample as well as the structural disaggregation and recovery under defined temperature and shear conditions are further examples.

At lower shear rates, moreover, the stroboscope can improve the quality of the microscopic images due to a shorter exposure time and a higher light intensity.<sup>7</sup> For direct comparison, microscopic images of an oil-in-oil

dispersion of silicone oil in mineral oil were recorded at three different shear rates using a cold light source (Fig. 4) or a stroboscope (Figs. 5–6). A x 20 lens and a plate/plate measuring geometry with a diameter of 35 mm and a measuring gap of  $50\text{ }\mu\text{m}$  were used, the surface of the rotor was polished.

Significant differences were already visible at shear rates of  $1290$  and  $2520\text{ s}^{-1}$ : The images taken with the stroboscope with a flash frequency of  $20\text{ Hz}$  (Fig. 5) had a significantly higher quality than those obtained with a cold light source (Fig. 4). With the same sample, evaluable microscopic images could be obtained up to a shear rate of  $44,000\text{ s}^{-1}$  (Fig. 6).



Fig. 3: Stroboscope (BVS-II Wotan, Polytec GmbH), equipped with a Xenon flash lamp, maximum flash frequency  $20\text{ Hz}$  ( $200\text{ Hz}$  with internal trigger).

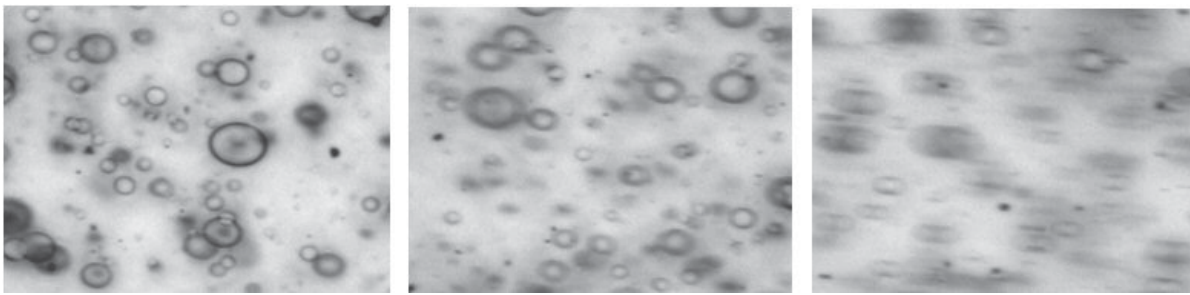


Fig. 4: Images taken at different shear rates using a cold light source:  $630\text{ s}^{-1}$  (left),  $1290\text{ s}^{-1}$  (center) and  $2520\text{ s}^{-1}$  (right).

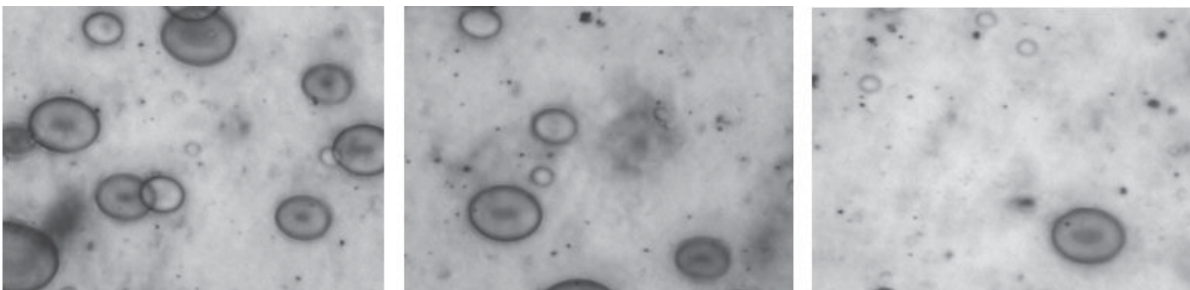


Fig. 5: Images taken at different shear rates using a stroboscope:  $630\text{ s}^{-1}$  (left),  $1290\text{ s}^{-1}$  (center) and  $2520\text{ s}^{-1}$  (right).

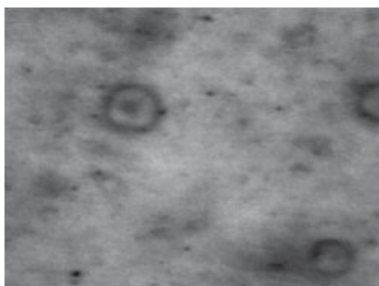


Fig. 6: Images taken at a shear rate of  $44,000\text{ s}^{-1}$  using a stroboscope.

### Contrast enhancing illumination

Samples with low optical contrast contain different components having similar refractive indices, e.g. oil-in-oil emulsions or chocolate melt/spread containing different kinds of fat. The quality of the regarding microscopic images can be improved significantly by adding a half circle diaphragm in the lighting tube.<sup>8</sup>

The required universal holder can be mounted easily as an additional segment either in the lighting tube and/or in the camera tube (Fig. 7) of any HAAKE RheoScope model. Moreover, these holders can be used for individual measuring set-ups with standard filters with a 12.5 mm metric thread, e.g. for wavelength-dependent investigations using color filters, long pass or short pass filters.<sup>8</sup>

Fig. 8 shows microscopic images (lens x 20) of a dispersion consisting of silicone oil S1000 (< 5 %) in mineral oil E6000 (> 95 %). A 35 mm plate/plate measuring geometry was used with a polished rotor surface and a measuring gap of 100  $\mu\text{m}$ . Comparing the images without (left) and with half circle diaphragm (right), a significant contrast enhancement can be seen — particularly for smaller droplets. This contrast enhancement improves also the accuracy of a subsequent particle size distribution determination, using an image analysis software, e.g. SPIP software.<sup>3</sup>

### Conclusion

Shear rates of 10,000  $\text{s}^{-1}$  and more can occur over shorter or longer times during processing and application of materials in coatings, food, pharmaceutical and cosmetic industry and can lead e.g. to breaking or coalescence of emulsions or other unwanted effects, causing a change in morphology and particle size distribution. The HAAKE MARS rheometer with HAAKE RheoScope module in combination with a stroboscope light source facilitates recording of sharp microscopic images at (very) high shear rates for formulation development, processing optimization and stability testing. By adding a half circle diaphragm in the lighting tube, the contrast of the images can be enhanced significantly.

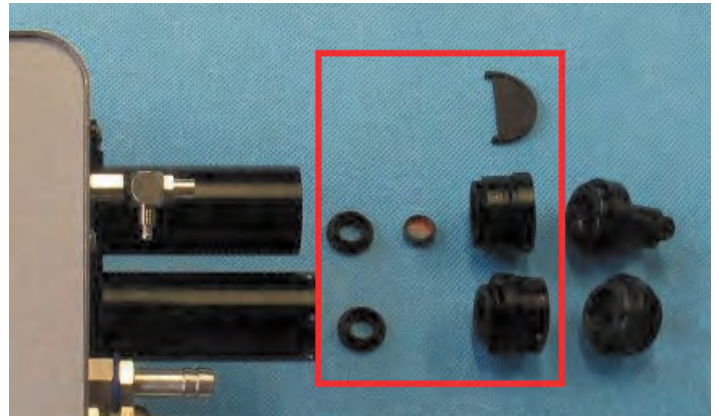


Fig. 7: Optional segment universal holder (red box) for HAAKE RheoScope lighting tube (center left) and/or camera tube (bottom left), offering a slit to mount a half circle diaphragm (top) as well as a mounting ring for a standard filter with a 12.5 mm metric thread (center).

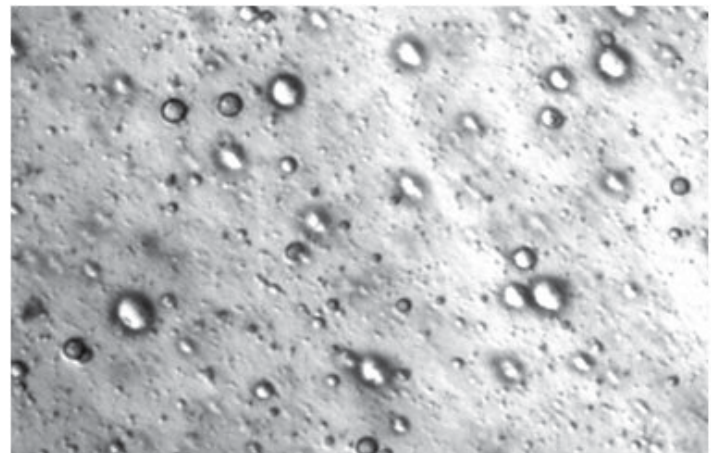
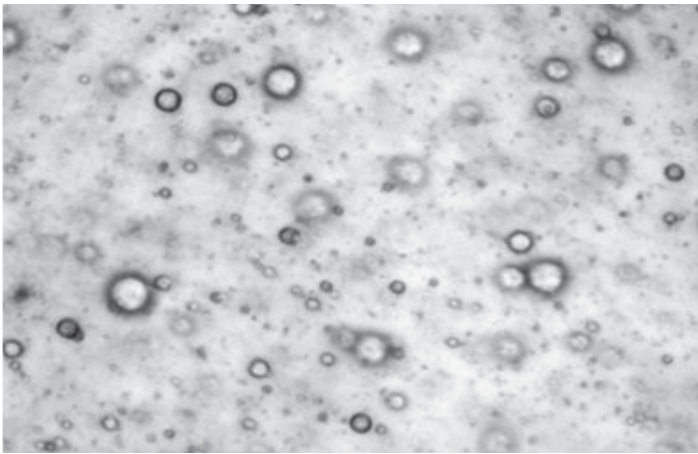


Fig. 8: Images taken on an oil-in-oil emulsion without (left) and with half circle diaphragm (right).

## References

1. Sugimoto K., Soergel F., Feustel M. Monitoring emulsions morphology under shear via simultaneous rheometry and in-situ FTIR spectroscopy, Thermo Scientific Application Note V-257 (2012)
2. Oldörp K. Strukturierung von Schäumen mittels Rheooptik. Tagungsband II. DGK-User Meeting „Rheologie kosmetischer Emulsionen“ 22.-23.10.08 Hamburg (2008)
3. Küchenmeister C., Sierró P., Soergel F. SPIP software for analysis of RheoScope images. Thermo Scientific Product Note P-009 (2009)
4. Oldörp K. What happens when rheological properties change? Looking into rheological properties with simultaneous collection of microscopic images. Thermo Scientific Application Note V-228 (2009)
5. Oldörp K. Waxing of crude oil – An easy approach with rheooptical methods. Thermo Scientific Application Note V-241 (2010)
6. Soergel F., Hauch D., Jährling M., Paulsen K., Weber- Kleemann A., Cech T., Gryczke A., Schmölzer S., Zecevic D. Investigation of pharmaceutical hot-melts via simultaneous rheometry and polarization microscopy, Thermo Scientific Application Note V-262 (2013)
7. Küchenmeister C., Soergel F. Thermo Scientific HAAKE RheoScope module: image acquisition at (very) high shear rates using a stroboscope light source. Thermo Scientific Product Note P-040 (2012)
8. Küchenmeister C., Soergel F. Thermo Scientific HAAKE RheoScope: Universal Holder for optical components for contrast enhancement and customized set-ups. Thermo Scientific Product Note P-042 (2013)

# Curing of an acrylate – Rheology with simultaneous FTIR spectroscopy

Author: Klaus Oldörp

## Introduction

Anybody who has ever worked with glues knows that timing is one of the crucial issues. Subsequently technical leaflets for glues sometimes look like timetables. Terms like pot life, open time, time for minor adjustments, curing time or time to reach maximum bonding strength, are used to describe the properties of glues and to give guidance for their successful application.

For the development of new glues such times have to fit the application to create a product that the target market will accept. For example, depending on the method to apply the glue, the open time needs to be adjusted to avoid curing before the parts have been joined.

A rheometer is an essential tool to characterize not only the uncured glue but especially the curing process itself. Regardless of whether a drying glue, a 2-component system, a thermally curing glue or a UV curing glue is investigated, the Thermo Scientific™ HAAKE™ MARS™ Rheometer and its wide range of accessories are the perfect tools to characterize curing behaviors.

Still, the classical limitation of rheological methods remains: a rheometer can only tell us what happens during the curing but it does not tell us why. The “why” becomes especially important when we want to understand why a batch of glue shows properties other than those expected or when we want to develop glue for a new application. To overcome this limitation, the rheological data needs to be combined with data from another analytical method able to detect what happens on the molecular scale. The molecular data provides the complementary „why“ information to the rheological measurements. A perfect



Figure 1: Setup with the HAAKE MARS Rheometer, Rheonaut module\* and FTIR spectrometer.

match is FTIR spectroscopy, a technique that can identify and quantify different chemical groups in a substance or in a mixture of substances.

Rheometers and spectrometers are two different types of analysis, each often with its own instrument. The disadvantage of running tests on two separate instruments is the extra effort it takes to prepare two different samples following different procedures for each method. Plus, as a consequence, this approach makes it virtually impossible to collect both sets of data on two identical samples under exactly the same conditions.

To combine rheological tests with FTIR spectroscopy without the aforementioned disadvantages, the Rheonaut module has been developed. This module is a unique combination of a temperature control module and an attenuated total reflection (ATR) cell with its own IR detector. With the Rheonaut module, the HAAKE MARS Rheometer can be combined with an FTIR spectrometer to one analytical setup (Figure 1). Only with this unique combination is it possible to record the mechanical changes of the curing glue while simultaneously and, even more importantly, collecting IR spectra on the same sample to track the chemical changes inside the sample.

## Experimental

A consumer-grade 2-component acrylate glue was prepared by mixing both components outside the rheometer according to its technical leaflet. Part of this mixture was transferred into the rheometer.

When designing the test method, two important facts about curing materials have to be kept in mind:

1. The curing reaction starts already outside the rheometer. To be able to compare different datasets, the test method contains an element to reset the internal time at the moment the 2 components start to be mixed (Figure 2, steps 3 and 4). Otherwise, any deviation in the loading procedure would lead to an undefined offset on the time axis.
2. The biggest changes happen during the first moments of the curing process. The test method has been optimized to start the test as quickly as possible after the sample is put onto the lower plate. The upper geometry is lowered to 10 mm before loading the sample to shorten the time to reach the measuring gap (Figure 2, step 6). The test itself starts immediately after the measuring gap has been reached without any time for thermal or mechanical equilibration.

The rheological part of the test method is an oscillation time curve (Figure 2, step 10) where the oscillation parameters are kept constant to detect only changes in the sample due to the curing. Since drastic changes of the moduli are expected during the test, the rheometer's controlled deformation (CD)-mode is used to ensure optimum signal quality throughout the whole test. A small amplitude within the sample's linear viscoelastic range (LVR) is selected, which still yields data with a good signal-to-noise-ratio from the uncured glue. The evaluation can be based on the storage modulus  $G'$  representing the elastic

part of the viscoelastic properties and the loss modulus  $G''$  representing the viscous part (Figure 3).

1		ID 2: Lift	Zero point; Lift apart
2		ID 3: FTIR spectrum	Configuration file   Background (reference) spectrum
3		ID 4: Message	Press ENTER when components start to mix
4		ID 5: Set / Reset	Reset total time
5		ID 6: Lift	Standby 10,000 mm
6		ID 7: Message	Load sample
7		ID 8: Set / Reset	Set angle position: optimal   Reset normal force
8		ID 9: Lift	Measurement position
9		ID 10: Set / Reset	Fn-set = 0,000 N   Stop if $ G^*  < 2000$ , Pa
10		ID 11: Osc Time	CD 0,1000 % f 1,000 Hz t 120,00 min #720 T 23,00 °C IRspectrum;

End of job

**Figure 2: Test method for 2-component glues shown in Thermo Scientific™ HAAKE™ RheoWin™ Measuring and Evaluation Software. In steps 3 and 4 the time is reset when the 2 components mix outside the rheometer. In step 5 the upper geometry moves to a 10 mm gap to minimize lift travel after the sample is put onto the lower plate. Step 8 moves the upper geometry to the measuring gap, and step 10 starts the test without waiting for temperature equilibration.**

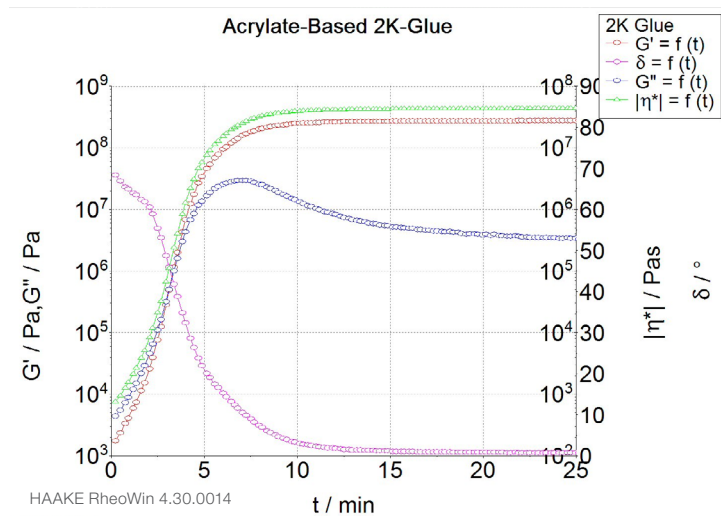


**Figure 3: Curing of an acrylate glue; development of the moduli  $G'$  and  $G''$ , the complex viscosity  $|\eta^*|$  and the phase angle  $\delta$  over time.**

The freshly prepared glue is mainly viscous;  $G''$  dominates over  $G'$  with phase angle ( $\delta$ ) values around  $70^\circ$  (purely viscous:  $\delta = 90^\circ$ , purely elastic:  $\delta = 0^\circ$ ). The curing reaction proceeds quickly; after 3.2 min the crossover point where  $G'' = G'$  or  $\delta = 45^\circ$  is reached. From this so-called gel time on, the glue behaves as mainly elastic because a wide meshed network has developed throughout the sample. Joining and fixing the two parts to be glued together has to be done well before the gel time is reached. Otherwise any movement in the glue line is either no longer possible or would reduce the final bonding strength. After 10 min



compared to reactions of the free monomer, which dominated the initial part of the curing.

With this information it is possible to understand why the curing process runs the way it does. Subsequently a targeted approach to optimize a glue or to design a completely new formulation is now possible. For example, it's known whether it would be better to add more monomer or to increase the temperature to increase the mobility of the existing monomer.

## Summary

An oscillation time sweep is a well-established method to characterize the curing of glues and similar curing materials. It shows the transition from the liquid to the solid state based on the mechanical properties of the glue. The rheological results can answer questions about the dosing and application properties of the liquid glue as well as the toughness of glue bond. The evaluation of the changing rheological properties gives the characteristic time spans like the pot life, the curing speed and the time to reach maximum strength of the bond.

Using the Rheonaut module, the HAAKE MARS Rheometer can be combined with an FTIR spectrometer to simultaneously record on the same sample what happens during the curing process and why it happens on a molecular level. This significantly reduces the time for sample preparation and analyses and excludes any uncertainties due to different sample composition or sample treatment when running both analyses separately.

The unique combination of rheological and spectroscopic methods not only increases the quality of the data collected but also increases the time efficiency and cost efficiency of an analysis like the one described in this report.

Find out more at [thermofisher.com/rheometers](https://thermofisher.com/rheometers)

# UV-induced curing reactions investigated by simultaneous rheometry FTIR measurements

Jan Philip Plog, Thermo Fisher Scientific, Karlsruhe, Germany

## Introduction

In many industrial segments the use of UV curing materials for the processing or application of paints, inks, adhesives, coatings, etc. is of utmost importance. This technology combines environmental and economical advantages with improved product features.

A curing process can be followed by dynamic rheological measurements, since the build-up of a network in the sample is directly related to the change of the viscoelastic properties ( $G'$ ,  $G''$ , etc.) of that sample.

By combining oscillatory rheological measurement with a second analytical technique an even more comprehensive insight into the characteristics of curing processes can be achieved. Such a supplemental tool can be e.g. FTIR spectroscopy. For a curing process or phase transition in general a rheometer can analyze the time dependent change of the viscoelastic properties of a material. The viscoelastic properties of a material however depend on its structure and especially its structural changes during a curing process. Infrared spectroscopy is an excellent tool for determining structural changes on a molecular level.

We will present technical details of new UV-curing set-up for the Thermo Scientific™ HAAKE™ MARS™ Rheometer and show the experimental results of the investigation of an UV-curing processes for an acrylate based coating for optical fibers. The presented data includes rheological as well as spectroscopic data.

## Measurement and set-up

With the patented\* Rheonaut module a standard FTIR spectrometer with side port and the HAAKE MARS Rheometer are coupled to form one measuring unit (Fig. 1).



Fig. 1: left: HAAKE MARS rheometer with Rheonaut module and FTIR spectrometer; right: HAAKE MARS rheometer configuration for UV-curing measurements incl. temperature control.



Fig. 2: left: measuring geometry and adapter for mounting and adjusting the collimator and light guide; middle: upper shaft with integrated mirror; right: holder for collimator plus closed hood.

For investigating UV curing materials with the Rheonaut module a new fixture for the HAAKE MARS Rheometer platform has been developed. This module consists of an upper shaft with an integrated mirror and an exchangeable quartz glass plate (Fig. 2), as well as a holder for a collimator plus light guide, which is mounted to the HAAKE MARS measuring head (Fig. 2). The UV light beam of a commercially available light source, first bundled by the collimator and then reflected by the mirror, is directed into the sample vertically from above through the quartz glass plate (Fig. 2). The quartz glass plate is the upper plate of a plate/plate measuring geometry, whereas the lower plate is either a standard temperature control module or the Rheonaut module for simultaneous measurements of rheological properties and FTIR spectroscopy.

The use of the optional available sample hood is recommended for measurements above ambient conditions. This hood is made of Teflon and can be used for temperatures up to 240 °C. This new setup enables the user to expose a material to UV-radiation while collecting rheological and spectroscopic data at the same time.

## Materials

The single glass fibers in an optical fiber cable are typically coated with a polymeric material to protect them from moisture and physical damage. The utilized coatings are usually UV-cured urethane acrylate composite materials applied to the outside of the fiber during the drawing process. In current practice, a dual layer coating system is used. These layers are applied at speeds of up to 1000 m/min. In order to optimize the final coating behavior and reduce the energy consumption during production a comprehensive understanding of the curing reaction is essential. In the following the rheological and spectroscopic investigation of the curing of an acrylate based coating formulation is shown.



Fig. 3: Uncoated optical fibers.

## Results

The following measurements were performed at 25 °C using the new UV curing cell in the HAAKE MARS III and the Rheonaut module for collecting the spectroscopic data. Fig. 4 shows the rheological data of the measurement of a UV-curing acrylate based glass fiber coating. The set strain value was 0.01. After the UV light source was triggered for the first time at 30 s  $G'$  and  $G''$  are increasing over several orders of magnitude. During the curing process the sample was exposed to UV light every two seconds for a period of one second.  $G'$  reaches its maximum after 100 s and remains constant for the rest of the experiment. After the initial increase  $G''$  runs through a maximum and decreases almost one order of magnitude before it reaches a plateau after 240 s. This behavior indicates a curing process in two steps. After the initial solidification the decrease of  $G''$  can be related to a further increase of the crosslink density. This second step has no influence on the evolution of  $G'$  or the overall stiffness of the material but rather on its brittleness. After 240 s no changes on the rheological parameters can be observed anymore and the curing reaction is completed.

Beside the rheological data the IR-spectra were collected during the experiment. The results are shown in Fig. 5. One of the advantages of FTIR spectroscopy is the high spectrum acquisition rate. Combined with the Fast Oscillation function of the RheoWin software even very rapid structural changes can be monitored in a rheological and spectroscopic way. Figure 5 shows three representative spectra taken before the uncured sample was exposed to UV-light, during the steep increase of the moduli and after  $G'$  and  $G''$  reached their plateau values. Some of the characteristic peaks are highlighted and shall be mentioned here. At  $1719\text{ cm}^{-1}$  and at  $1179\text{ cm}^{-1}$  decreasing peaks are observed.

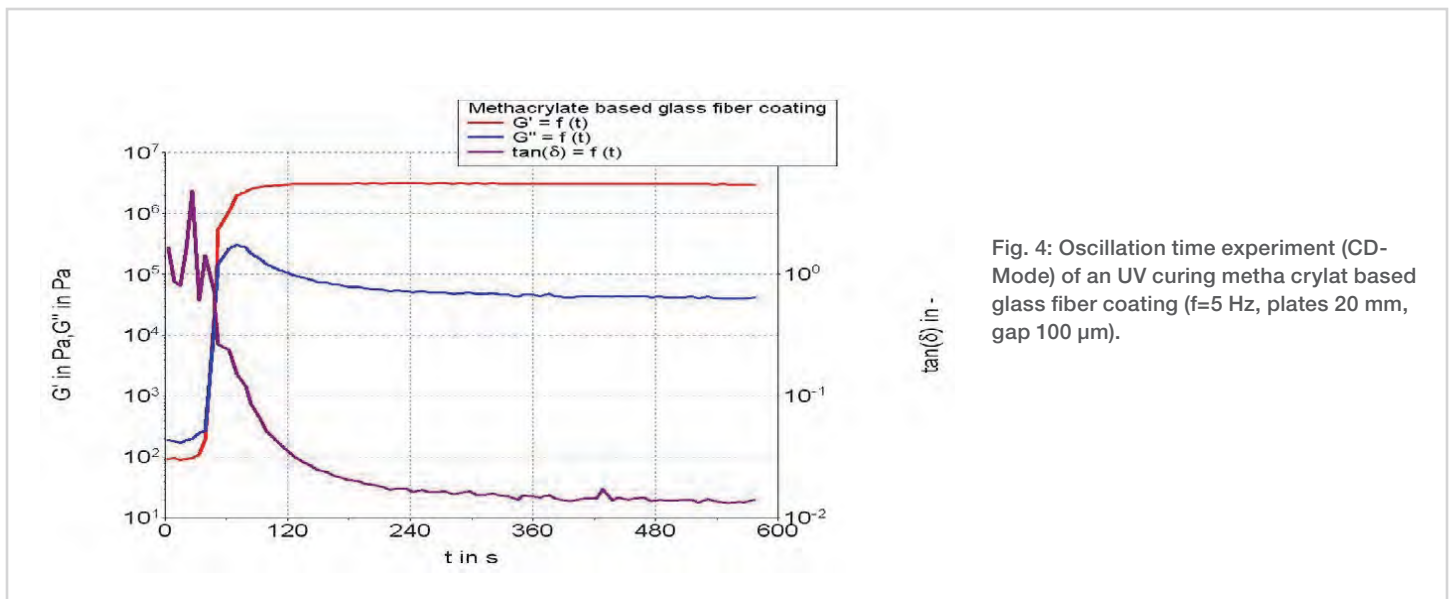


Fig. 4: Oscillation time experiment (CD-Mode) of an UV curing metha crylat based glass fiber coating ( $f=5\text{ Hz}$ , plates 20 mm, gap 100  $\mu\text{m}$ ).

These are characteristic wavelength numbers for stretching vibration of carbonyl groups. Therefore it can be concluded that this functional group is actively involved in the curing process and the amount of free carbonyl groups is decreasing over time. Another characteristic peak that stands out in the presented spectra is at  $808\text{ cm}^{-1}$ . At this wavenumber  $\text{=C-H}$  groups transform absorbed energy into bending vibrations.

The mentioned examples demonstrate how the structural changes within a curing sample can be monitored and evaluated on a molecular level. Along with the rheological information gained from the oscillatory experiment, this combined measuring technique provides a comprehensive insight into complex processes. Therefore it can be an ideal tool for optimizing industrial curing processes with regards to sample performance and energy efficiency.

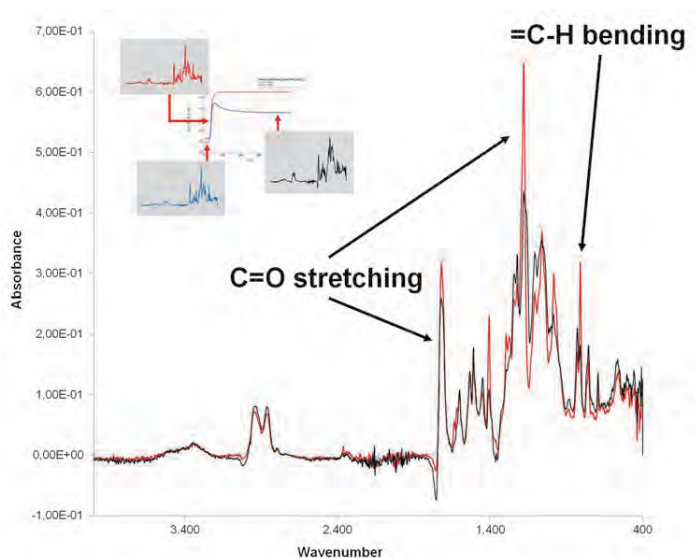


Fig. 5: IR-Spectroscopic data of acrylate based coating formulation before while and after being exposed to UV-light.

Find out more at [thermofisher.com/rheometers](https://thermofisher.com/rheometers)

# Rheology-Raman Spectroscopy: Tracking emulsion stability with the combination of a rheometer and Raman spectrometer

Jan P. Plog<sup>a</sup> and Matthew Meyer<sup>b</sup>

<sup>a</sup>Thermo Fisher Scientific, Karlsruhe, Germany | <sup>b</sup>Thermo Fisher Scientific, Madison, USA

## Introduction

As the stress-strain response of complex fluids is closely linked to changes in physical or chemical structure within the material, rheology can be most useful when combined with simultaneous measurement of physical or chemical properties affecting flow.

Chemical information including molecular conformation, bond formation or scission, and chemical composition is also critically relevant to rheological measurements. Vibrational spectroscopic tools such as Raman spectroscopy have proven to be powerful noninvasive techniques to probe chemical information of interest in a variety of soft matter systems including emulsions.<sup>1</sup>

The benefit of simultaneous measurements is clear: many soft materials are sensitive to temperature and flow history, so simultaneous measurements minimize experimental variation.

In this application note, we present results obtained on a cosmetic emulsion in cooperation with NIST published previously.<sup>2</sup>

The results shown can be obtained with the brand new combination of a Thermo Scientific™ HAAKE™ MARS™ Rheometer with a Thermo Scientific™ iXR Raman Spectrometer (Thermo Scientific™ HAAKE MARS<sub>XR</sub> RheoRaman System) as shown in Fig. 1.



Fig. 1: HAAKE MARS<sub>XR</sub> RheoRaman System

## Result and discussion

The experimental setup shown in Fig. 1 represents a novel integration of commercial instrumentation: a Raman spectrometer (Thermo Scientific iXR Raman) and rotational rheometer (HAAKE MARS) are coupled through an optically transparent base modified from the Thermo Scientific™ RheoScope Module.

The cosmetic emulsion tested consists of oil droplets suspended in water and is stabilized by a mixture of surfactants. The Raman spectra of the emulsion over the spectral range at 25 °C is shown in Fig. 2a. The broad peak in the range of 200 cm<sup>-1</sup> to 600 cm<sup>-1</sup> is attributed to the fused silica window between the objective and the sample. Additionally, a small sharp band at 2330 cm<sup>-1</sup> is due to ambient nitrogen. A number of peaks are observed in the fingerprint region of 650 cm<sup>-1</sup> to 1600 cm<sup>-1</sup> and are magnified in Fig. 2b. Although a complete chemical component analysis based on the measured spectra is

outside the scope of this application note, the sharp peaks in the fingerprint region appear at positions attributed to the vibrational bonds of alkyl groups  $C_nH_{2n+1}$ : the C-C symmetric and asymmetric stretch peaks at  $1063\text{ cm}^{-1}$  and  $1130\text{ cm}^{-1}$  respectively, the  $CH_2$  twist mode at  $1296\text{ cm}^{-1}$ , and multiple modes associated with  $CH_2$  bending motion at  $1418\text{ cm}^{-1}$ ,  $1441\text{ cm}^{-1}$ , and  $1464\text{ cm}^{-1}$ .

These alkyl group modes are present due to the alkyl chains present on the stabilizers and fatty acids comprising the majority of the coconut and almond oils in the emulsion. The broad distribution of Raman bands in the range of  $750\text{ cm}^{-1}$  to  $950\text{ cm}^{-1}$  is common for C-O-C stretch modes expected for the polyethylene oxide groups present in polysorbate  $CH_2$  rocking modes for fatty acids and alcohols.<sup>3</sup> The presence of methyl  $CH_2$  groups is further evidenced by the presence of peaks in the  $2600\text{ cm}^{-1}$  to  $3000\text{ cm}^{-1}$  region (shown in greater detail in Fig. 2c) attributed to  $CH_2$  and  $CH_3$  stretching modes.

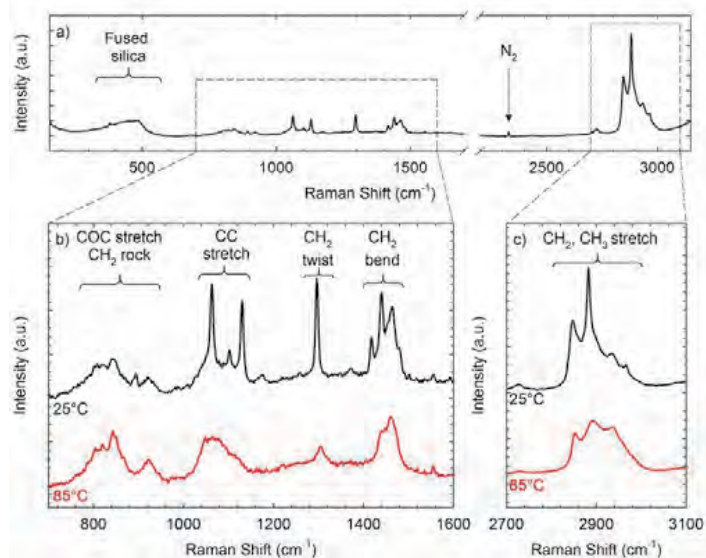


Fig. 2: (a) Raman spectra of the emulsion at room temperature over the instrument range. (b) Raman spectra of the emulsion in the range of ( $700$  to  $1600$ )  $cm^{-1}$  at temperatures indicated in the figure. (c) The same spectra collected in (b) in the ( $2700$  to  $3100$ )  $cm^{-1}$  region. Note that the intensity scaling varies from (b) to (c).

Upon heating, the sharp peaks due to the C-C stretch,  $CH_2$  twist, and  $CH_2$  bend modes decrease in intensity relative to broader peaks in the spectra as shown in Fig. 2b. A similar loss of intensity of the sharp peak at  $2883\text{ cm}^{-1}$  in Fig. 2c is evident at the higher temperature. The loss of intensity in these peaks corresponds to increasing conformational disorder along the alkyl chains present in the stabilizer, fatty acid, and fatty alcohol chains due to melting.

Quantitative measurement of alkyl chain measurement can be obtained by analysis of the peaks associated with the  $CH_2$  twisting modes.<sup>4</sup> Our analysis of the spectra in the

$CH_2$  twist region follows a similar protocol used to quantify consecutive trans and amorphous conformers in alkanes and polyethylenes.<sup>5</sup> The Raman spectra are fit using two Lorentzian peaks: a narrow peak of approximately  $2\text{ cm}^{-1}$  FWHM centered at  $1296\text{ cm}^{-1}$  and a broader peak of approximately  $13\text{ cm}^{-1}$  FWHM at  $1303\text{ cm}^{-1}$ . These fits are used to calculate the integrated area  $I$  of each peak. The total area under the curves in the  $CH_2$  twist region  $I_{1296} + I_{1303}$  is invariant with respect to chain disorder, which provides a method to normalize the spectra. The area of the peak at  $1296\text{ cm}^{-1}$  normalized by the total area then quantifies the mass fraction of chains with more than four consecutive trans sequences along the chain. The value of  $I'$  quantifies the mass fraction of ordered chains.

$$I' = \frac{I_{1296}}{(I_{1296} + I_{1303})}$$

Simultaneous Raman and viscosity measurements of the emulsion are shown in Fig. 3 for the temperature ramp from  $25\text{ }^{\circ}C$  to  $90\text{ }^{\circ}C$  at a rate of  $1\text{ }^{\circ}C/min$ . The viscosity is measured at a steady shear rate of  $30\text{ s}^{-1}$  and a gap thickness of  $200\text{ }\mu m$ . Lower shear rates lead to shear localization in a thin fluid layer between the rotor and the droplet phase, which is confirmed via polarized optical imaging of immobile droplets in the bulk (however, this phenomenon is beyond the scope of this manuscript.) The viscosity decreases with increasing temperature until approximately  $50\text{ }^{\circ}C$ , at which point the viscosity sharply decreases.

The temperature range of  $45\text{ }^{\circ}C$  to  $55\text{ }^{\circ}C$  where viscosity and *consecutive* trans fraction exhibit a strong temperature dependence, correlates well with the melting temperatures of stabilizers in the emulsion including cetyl alcohol and stearyl ammonium chloride. These simultaneous measurements allow for clear correlation of steady shear viscosity with conformational information.

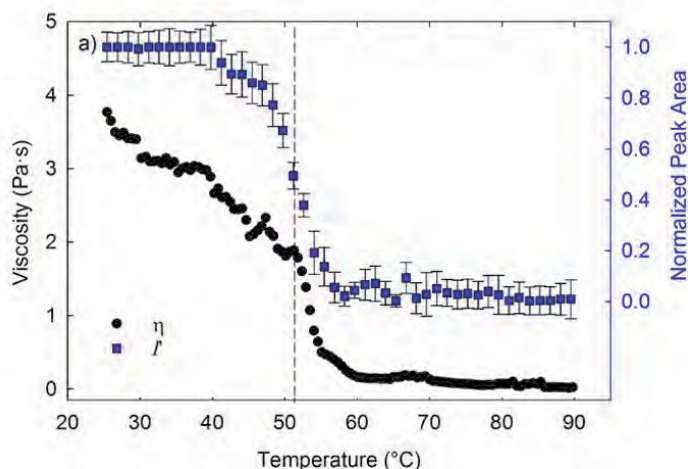


Fig. 3: Viscosity and normalized peak area  $I'$  as a function of temperature for the emulsion.

## Summary

With the Thermo Scientific HAAKE MARS<sub>XR</sub> RheoRaman System, simultaneous measurements of rheological properties and Raman-active molecular vibrations are possible. The emulsion example shown in this work, highlights the applicability of the MARS<sub>XR</sub> to characterize structural and conformational changes directly related to the rheological response of the material. Since all measurements are performed simultaneously, experimental conditions such as temperature and flow history are identical for Raman and rheology. In addition, the laser excitation and collection path can be equipped with optical elements for polarized Raman measurements. Based on the possibilities for direct correlation between chemical, structural, and mechanical properties, we expect the MARS<sub>XR</sub> to be critically relevant to both academic and industrial interests.

## References

1. M. Amer, Raman spectroscopy for soft matter applications (John Wiley & Sons, 2009).
2. A. P. Kotula et. al., Review of Scientific Instruments 87, 105105 (2016).
3. J. De Gelder, K. De Gussem, P. Vandenabeele and L. Moens, J. Raman Spectrosc. 38, (2007).
4. K. G. Brown, E. Bicknell-Brown and M. Ladjaj, J. Phys. Chem. 91, (1987).
5. K. B. Migler, A. P. Kotula and A. R. Hight Walker, Macromolecules 48, (2015).

Find out more at [thermofisher.com/rheometers](https://thermofisher.com/rheometers) and [thermofisher.com/msr](https://thermofisher.com/msr)

**ThermoFisher**  
SCIENTIFIC

# Rheology-Raman Spectroscopy: Tracking polymer crystallization with the combination of a rheometer and Raman spectrometer

Jan P. Plog<sup>a</sup> and Matthew Meyer<sup>b</sup>

<sup>a</sup>Thermo Fisher Scientific, Karlsruhe, Germany | <sup>b</sup>Thermo Fisher Scientific, Madison, USA

## Introduction

The use of a coupled rheometer and Raman spectrometer for obtaining comprehensive insight into a materials behavior is presented in this application report.

Rheology is the analytical method of choice to correlate the absolute flow and deformation characteristics of a given product with its behavior towards a certain processing or application step. However, Rheology as an integral method only yields answers on the bulk of the investigated sample. It does not give any insights into what is actually happening on the molecular level during a certain processing step.

Raman spectroscopy has shown its ability as a powerful, effective and non-invasive method for chemical analysis. Coupling a rheometer with a Raman spectrometer provides direct information about the molecular structure and the mechanical properties. This is extremely useful for studying the crystallization behavior of polymer melts during processing. It can also provide insight for *in-situ* characterization and monitoring which can be challenging when working with on-line techniques as only relative flow fields are characterized.

In this application note, we present results obtained on an HDPE melt in cooperation with NIST published previously.<sup>1</sup>

The results shown can be obtained with the brand new combination of a Thermo Scientific™ HAAKE™ MARS™



Fig. 1: HAAKE MARS<sub>xR</sub> RheoRaman System

Rheometer with a Thermo Scientific™ iXR Raman Spectrometer (Thermo Scientific™ HAAKE MARS<sub>xR</sub> RheoRaman System) as shown in Fig. 1.

## Result and discussion

Melting and crystallization are two common phase transitions that are critical to the flow properties of various complex fluids. These temperature-sensitive transitions are often indicated via changes in molecular conformation, while optical measurements provide direct observation of structural characteristics. However, measurements performed on separate instruments are often challenging to correlate due to variations between samples, processing history, and temperature control. To demonstrate the capabilities of the MARS<sub>xR</sub>, we provide simultaneous Raman and rheological measurements on high density polyethylene (SRM 1475, National Institute of Standards and Technology, Gaithersburg, MD) during crystallization.

The experimental setup shown in Fig. 1 represents a novel integration of commercial instrumentation: a Raman spectrometer (Thermo Scientific iXR) and rotational rheometer (HAAKE MARS) are coupled through an optically transparent base modified from the Thermo Scientific™ RheoScope Module. To monitor crystallinity one has to have a look at the Raman spectra for HDPE as shown in Fig. 2.

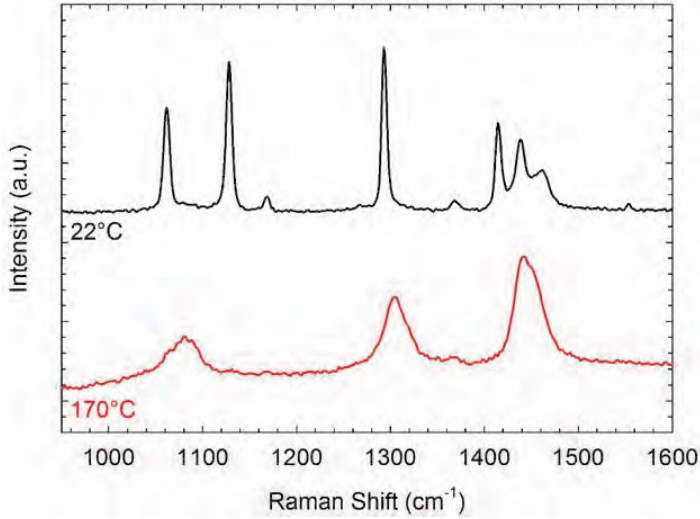


Fig. 2: Raman spectra of polyethylene at temperatures corresponding to the semi-crystalline state (22 °C) and the amorphous state (170 °C).

The spectrum at room temperature shows sharp peaks corresponding to the C-C stretch, CH<sub>2</sub> twist, and CH<sub>2</sub> bend. At 170 °C HDPE is in the melt state, and the sharp peaks are replaced with broader spectral features.

The Raman spectra of HDPE can be analyzed to quantify the crystallinity of the sample. Specifically, the area under the peak at 1416 cm<sup>-1</sup> in the HDPE spectra is directly proportional to the mass fraction of crystallinity in the sample. In order to calculate the crystallinity, the integrated peak area  $I_{1416}$  is normalized by the total area under the peaks in the CH<sub>2</sub> twist region and a scale factor  $N_c$ .

$$\alpha_{cr} = \frac{I_{1416}}{(I_{1296} + I_{1303}) N_c}$$

The scale factor  $N_c$  is a ratio of  $I_{1416}/(I_{1296} + I_{1303})$  for an HDPE sample to the crystallinity of that sample measured via DSC.

For HDPE on the MARS<sub>XR</sub>, the measured scale factor is  $N_c = 0.80 \pm 0.03$ . Although this is larger than calculated values of  $N_c$  from our prior measurements,<sup>2</sup> the Raman peak intensities of HDPE (and therefore the scale factor values) are strongly dependent upon the polarization state of the incoming and collected light as well as the scattering

angle.<sup>3</sup> The crystallinity for the room temperature sample in Fig. 2 is  $(73 \pm 4)\%$  which agrees with the crystallinity value of  $(74 \pm 5)\%$  measured via DSC.

The structure-property relationships during polymer crystallization are of critical interest and can be studied simultaneously using the MARS<sub>XR</sub>. An HDPE sample of thickness 750 μm was heated for 5 minutes at 155 °C, cooled at 10 °C/min to 134 °C, and then cooled at a slower rate of 2 °C/min to 124 °C and held at temperature to crystallize.

Fig. 3 shows simultaneous rheological and Raman measurements during HDPE crystallization. The complex modulus is measured during small-amplitude oscillatory shear using a fixed strain amplitude of 0.01 and oscillation frequency of 2π rad/s. Fig. 3 shows that early times in the crystallization process are characterized by  $G' < G''$ , but over time a crossover occurs in the modulus as the values of  $G'$  and  $G''$  increase over 2 orders of magnitude. The plateau in  $G'$  and  $G''$  at later times indicates the cessation of crystallization as measured by the complex modulus.

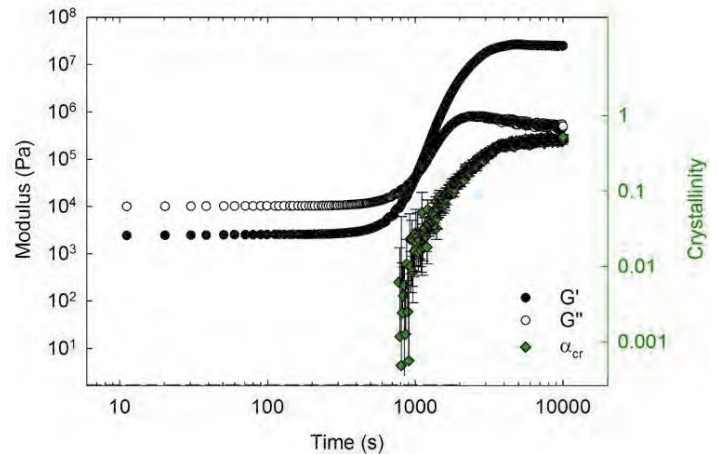


Fig. 3: Complex modulus and crystallinity of PE versus time during isothermal crystallization at 124 °C.

Raman spectra measured during the crystallization process are used to calculate the crystallinity of the sample via Equation 1.

Fig. 3 shows the instantaneous mass fraction of crystalline material, which first exceeds the measurement noise at approximately 800 s and increases over time. The appearance and increase in crystallinity as measured by Raman spectroscopy correlates with the increase in the complex modulus near the crossover point. Phase transition in the SRM 1475 is thus clearly driven by crystallization.

## Summary

Relating Raman and rheological measurements would be difficult on multiple instruments due to the sensitivity of the crystallization process on temperature, but using the MARSXR we can clearly correlate changes in the complex modulus with structural and conformational changes in the crystallizing HDPE melt.

## References

1. A. P. Kotula et. al., Review of Scientific Instruments 87, 105105 (2016).
2. K. B. Migler, A. P. Kotula and A. R. Hight Walker, Macromolecules 48, (2015).
3. P. J. Hendra, H. P. Jobic, E. P. Marsden and D. Bloor, Spectrochim. Acta, Part A 33, (1977).

Find out more at [thermofisher.com/rheometers](https://thermofisher.com/rheometers) and [thermofisher.com/msr](https://thermofisher.com/msr)

**ThermoFisher**  
SCIENTIFIC

# Tracking crystallization of EVA/acetaminophen mixtures with the combination of a rheometer and a Raman spectrometer

Jan P. Plog<sup>a</sup> and Massimiliano Rocchia<sup>b</sup>

<sup>a</sup>Thermo Fisher Scientific, Karlsruhe, Germany | <sup>b</sup>Thermo Fisher Scientific, Rodano, Italy

## Introduction

Hyphenated rheometry and Raman spectroscopy is presented in this application report as an analytical method to monitor the crystallization behavior of ethylene vinyl acetate (EVA) with and without acetaminophen.

Over the last few years there has been a growing demand from the pharmaceutical industry for EVA as a drug eluting excipient to be used in biomedical engineering as well as in hot melt extrusion (HME) applications. As shown in other works, EVA is an especially suitable excipient for low temperature HME thus enabling it to process active pharmaceutical ingredients (APIs) with low thermal stability.<sup>1</sup>

HME has been used extensively in the polymer industry to produce a wide range of plastic products in a variety of forms. However, HME applied to the production of pharmaceutical formulations is a relatively new method being developed as an attractive alternative to traditional batch processing methods for tablets, granules, pellets, and even transdermal films. The biggest advantage of HME is that as a continuous process, it allows for direct in-line monitoring and control of the manufacturing process.

HME is an easier way than traditional methods to produce a variety of different dosage formulations, generating product that can have enhanced dissolution, improved product delivery, and controlled release. During HME, a dry blend of the respective API and a thermoplastic excipient is



Fig. 1: HAAKE MARS<sub>xR</sub> RheoRaman System

melt-mixed using extruders. In the ideal case this leads to the formation of thermodynamically stable solid solutions or dispersions, which may provide for extended product lifetimes. One parameter that has a vast influence on final product stability as well as bioavailability of the API is the crystallinity of the thermoplastic excipient as well as the API.<sup>2</sup> As the crystallization of a given thermoplastic can be induced thermally and/or via applying shear stresses in the extruder, investigating the behavior prior to conducting large-scale HME experiments is beneficial. Also, it's necessary to understand whether the solid solution of API and thermoplastic stays thermodynamically stable after the manufacturing step or whether recrystallization of the API will occur. To investigate thermodynamic stability behavior on a lab scale the Thermo Scientific™ HAAKE™ MARS<sub>xR</sub> RheoRaman system can be used. This system is the hyphenation of a Thermo Scientific™ HAAKE™ MARS™ rheometer and a Thermo Scientific™ iXR™ Raman spectrometer. The system used for the work in this application report is shown in Fig.1.

## Results and discussion

To demonstrate the capabilities of the HAAKE MARS<sub>XR</sub> system, we provide simultaneous Raman and rheological measurements on ethylene vinyl acetate copolymer (28% VA) in pure form as well as mixed with acetaminophen (40 wt.%) during a variety of temperature sweep experiments in SAOS (small amplitude oscillatory shear). All rheological tests were conducted with a 35 mm parallel plate geometry at a gap of 750  $\mu\text{m}$  in CD oscillation at a strain amplitude of 1% and an angular frequency of 6.28 rad/s. Raman spectroscopy measurements were performed using the iXR Raman Spectrometer and the Thermo Scientific™ OMNIC™ Series spectroscopy software. The iXR system was equipped with a CCD camera cooled to  $-50\text{ }^{\circ}\text{C}$ , a triplet spectrograph providing Raman spectra over the range of 3500 to 50  $\text{cm}^{-1}$  Raman shift (Stokes) at 5  $\text{cm}^{-1}$  resolution and a 532 nm laser. A laser power of 10 mW was used on the sample to monitor the crystallization kinetic of EVA. Alignment of the laser, Raman scatter, and aperture selection within the spectrometer were all software controlled. The crystallization kinetic was monitored continuously starting from 120  $^{\circ}\text{C}$  with the melt polymer (see details in text below), by collecting spectra every 30 seconds (6 s exposure time for 5 accumulations).

The hyphenated system setup shown in Fig. 1 represents a novel integration of instrumentation: a Raman spectrometer and a rotational rheometer are coupled through an optically

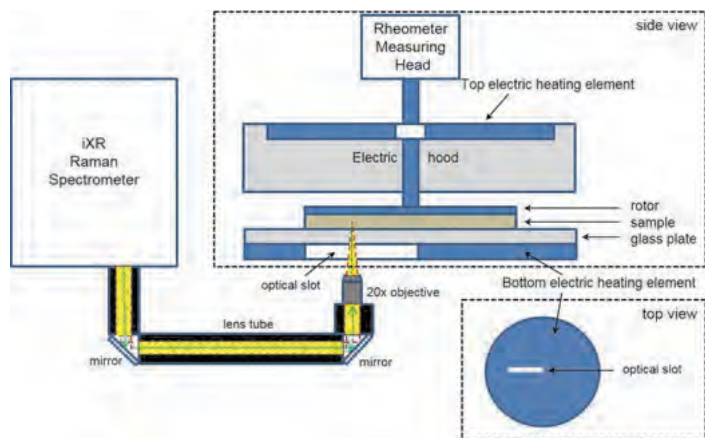


Fig. 2: Schematic view of the optical path from the Raman spectrometer into the rheometer.

transparent base modified from the Thermo Scientific™ RheoScope Module. A schematic of the setup is shown in Fig. 2.

To monitor the temperature influence on the crystallization behavior of the pure EVA, different temperature ramps were run on the rheometer as shown in Fig. 3. For each of the three runs, fresh sample was filled in the rheometer at 120  $^{\circ}\text{C}$ . Waiting time for melting of the sample was 10 min., then the gap was achieved and the sample was trimmed. After another 5 min of equilibration time the temperature was ramped down from 120  $^{\circ}\text{C}$  to 60, 65 and 70  $^{\circ}\text{C}$ , respectively, at a rate of 2 K/min. After reaching the final temperature, the sample was tested isothermally for another 20 to 30 min.

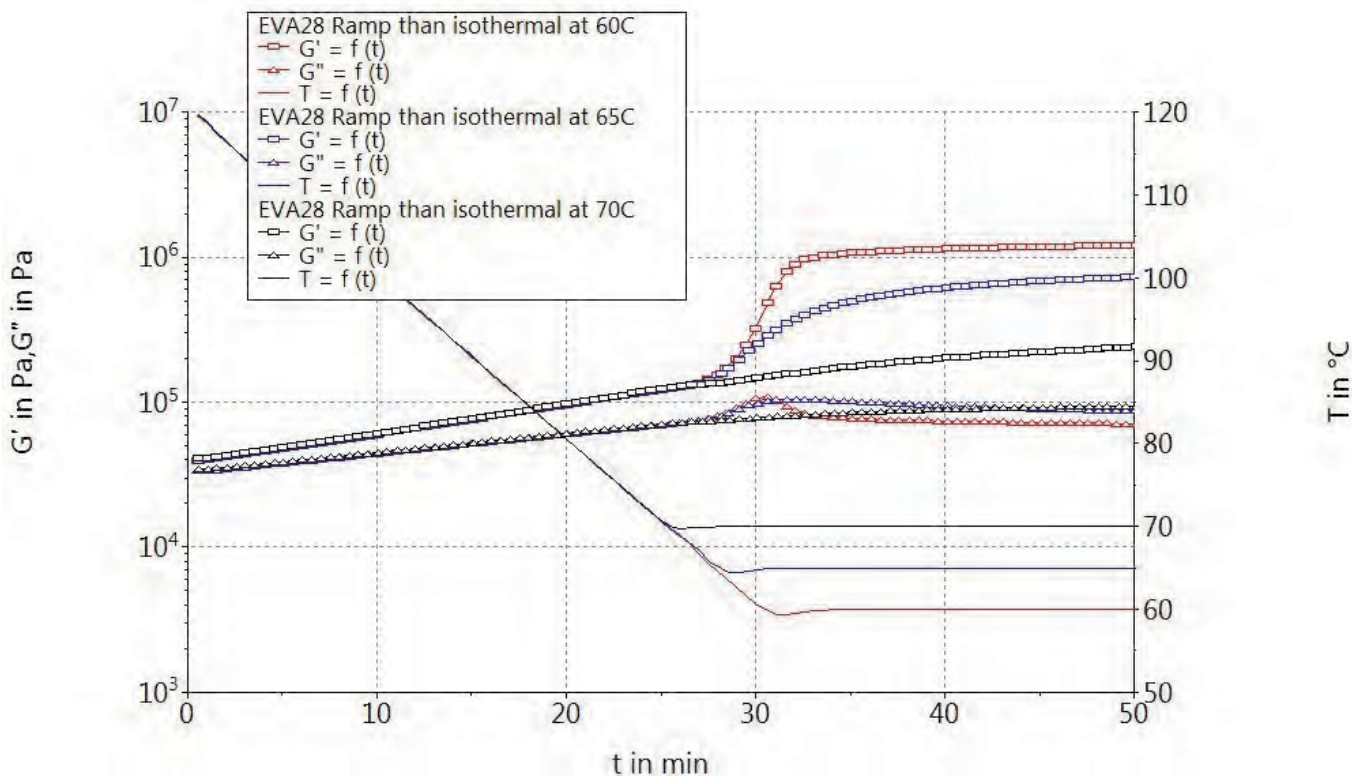


Fig. 3:  $G'$  and  $G''$  as a function of time and temperature for the pure EVA.

As can be seen from Fig. 3, the three data sets are congruent up to the isothermal stage. At 70 °C the EVA does not show a phase transition at all, whereas at 60 °C and 65 °C the EVA shows crystallization. The phase transition follows a faster kinetic at 60 °C compared to 65 °C, and higher  $G'$  values are reached at 60 °C with a smaller  $G''$  resulting in a smaller damping function  $\tan \delta (G''/G')$ . The behavior shown in Fig. 3 is supported by the simultaneously recorded Raman spectra as described below.

Fig. 4 shows the Raman spectra of the pure EVA in the molten phase at 120 °C just before starting the ramp down to reach the isothermal crystallization temperature of choice in comparison with the solid phase spectrum collected at room temperature.

As expected, considering the above interpretations, the Raman spectrum of the molten polymer does not exhibit peaks at 1416  $\text{cm}^{-1}$  and 1060  $\text{cm}^{-1}$  while it shows a prominent peak at 1079  $\text{cm}^{-1}$  relative to the disorder and amorphous content (Fig. 4). For more details on Raman spectroscopy for polyethylene, please refer to Thermo Fisher Scientific application note.<sup>3</sup>

As can be seen from Fig. 5A, the ratio of the intensities 1060/1079  $\text{cm}^{-1}$  (higher values of the ratio are indicative of a phase transformation and higher order) of the two data sets collected at 60 °C and 65 °C increase at the time of the phase transition and mimic the rheological data. The steeper slope observed for the isothermal crystallization conducted at 60 °C indicates that the kinetic of chain alignment is faster than at 65 °C, again in agreement with the rheological data. Whereas at 70 °C no phase transition is observed, the EVA stays molten at this point.

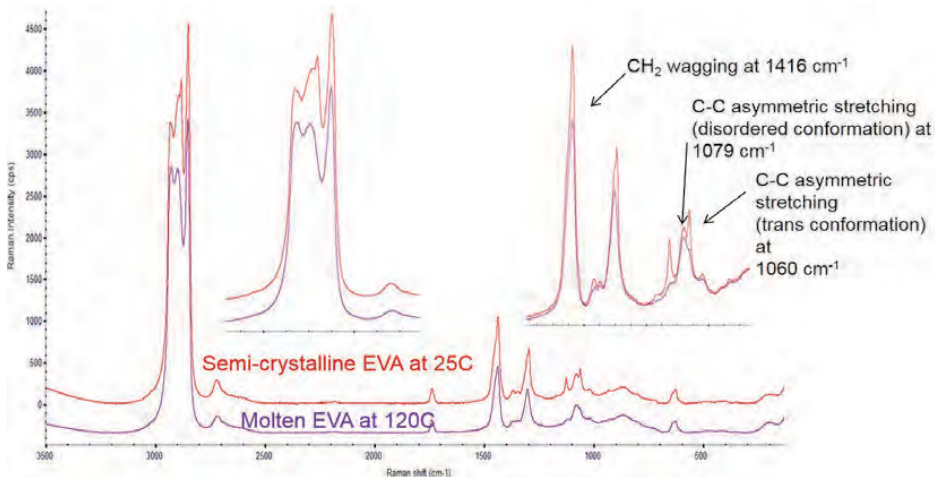


Fig. 4: Raman spectra of the pure EVA in molten (blue spectrum) and in the solid (red spectrum); the insets show a magnification of the most interesting region.

Wavenumber $\text{cm}^{-1}$	Mode	Correlating weight fraction
1416	-CH <sub>2</sub> Wagging	Crystalline Phase
1079	C-C Asymmetric Stretching (Conformational Disorder)	Amorphous Phase
1060	C-C Asymmetric Stretching (Consecutive Trans)	Ordered Phase

Table 1: Relevant polyethylen Raman bands for EVA28

The crystallinity peak, see Fig. 5B, shows very much the same behavior as the ratio, however the crystalline weight fraction at 60 °C is only marginally larger than at 65 °C.

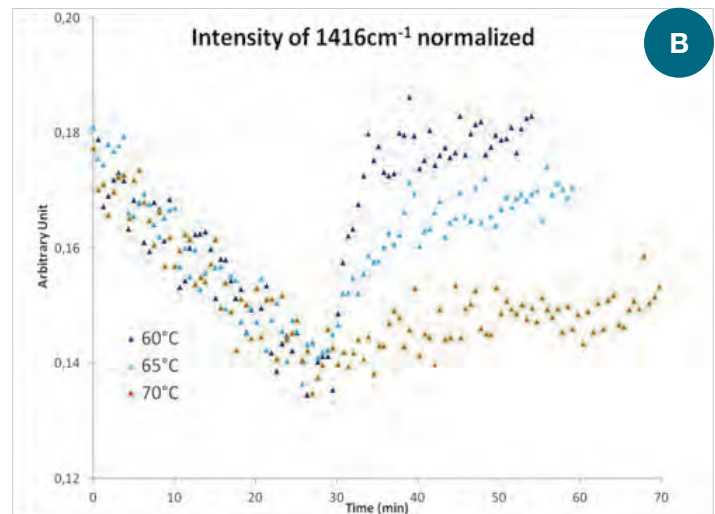
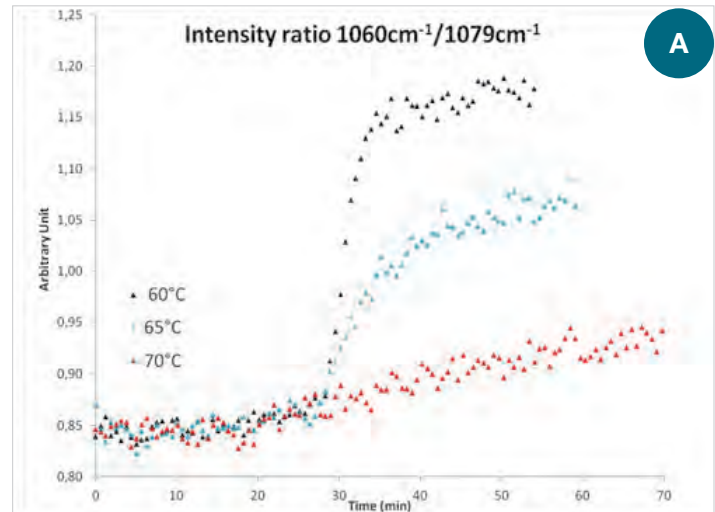


Fig. 5: Intensity ratio 1060  $\text{cm}^{-1}$ /1079  $\text{cm}^{-1}$  (A) and the intensity of the normalized peak at 1416  $\text{cm}^{-1}$  (B) for EVA at 60, 65 and 70 °C.

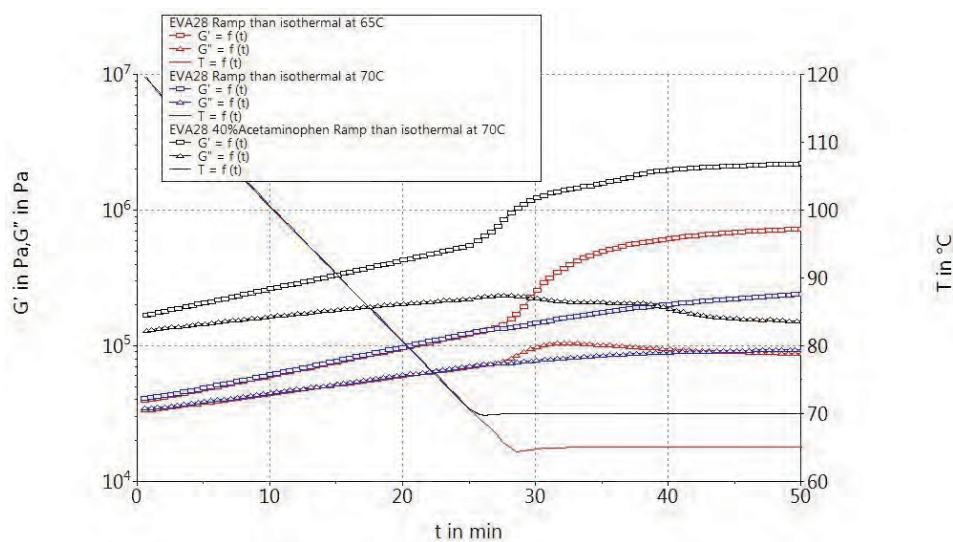


Fig. 6:  $G'$  and  $G''$  as a function of time and temperature for the pure EVA in comparison to the EVA/acetaminophen mixture.

Adding 40 wt.% of acetaminophen to the EVA changes the viscoelasticity and phase transition drastically (Fig. 6). The EVA/acetaminophen blend does not only exhibit higher viscoelastic moduli at higher temperatures, but also shows a phase transition at 70 °C in contrast to the neat EVA. Also, the EVA/acetaminophen blend shows an earlier transition than even the neat EVA did at 65 °C. Showing an even smaller value in the damping function  $\tan \delta$  emphasizes the fact that the added API leads to an overall much more brittle behavior arising from pronounced crystallization.

From the simultaneously collected Raman spectra in Fig. 7 one can come to the same conclusion as was derived from the rheological data: the addition of acetaminophen influences the crystallization behavior of EVA and causes a phase transition at 70 °C. Monitoring the intensity of the crystalline peak (Fig. 7B) provides further information. Clearly, in the case of added API, the phase transition starts 15 min earlier as compared to the neat EVA at 65 °C. The degree of crystallinity at the end of the isothermal process is higher in the EVA/ acetaminophen melt-blend as well.

Another valuable piece of information the Raman spectrum reveals is related to the morphology of the API, i.e. changes of the polymorph form of the acetaminophen in the compound caused by the exposure to elevated temperatures during the HME process. Fig. 8 shows the comparison of the spectra of the pure acetaminophen and the acetaminophen melt-blended with EVA at the end of the crystallization process. The Raman spectrum of the pure acetaminophen (blue spectrum in Fig. 8) can be assigned to the monoclinic form, the most common in commercial product and the most stable thermodynamically. After the process the acetaminophen (red spectrum) does not change form, but slight differences in relative intensities and peak positions in some regions of the spectra are observed. This may be

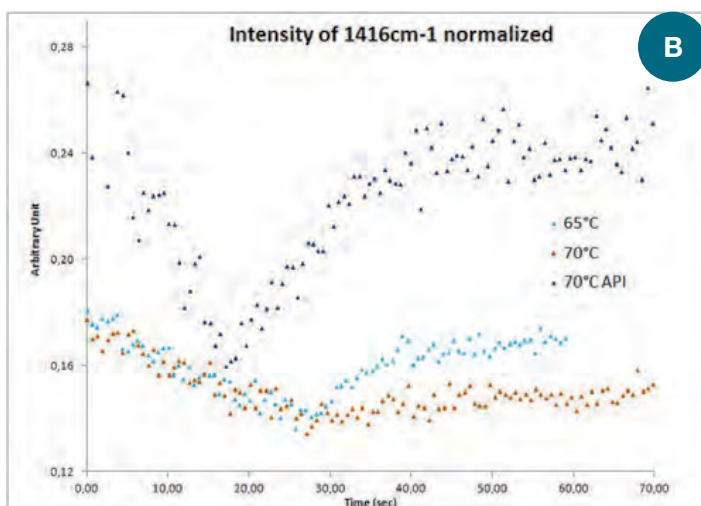
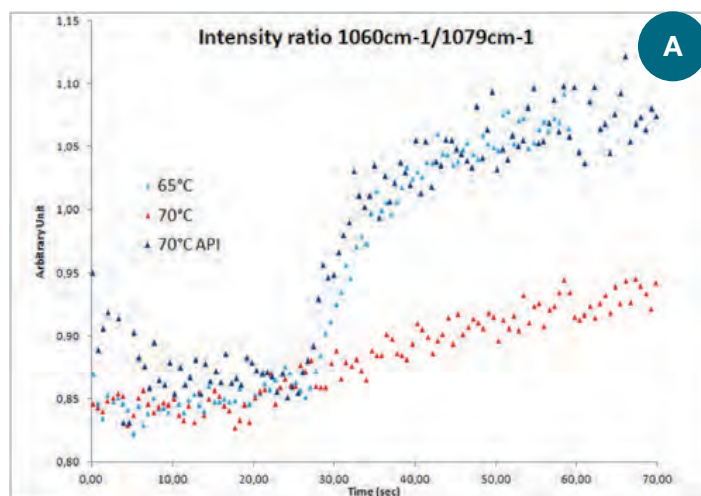


Fig. 7: Intensity ratio 1060  $\text{cm}^{-1}/1079\text{cm}^{-1}$  (A) and the intensity of the normalized peak at 1416  $\text{cm}^{-1}$  (B) for EVA at 65 and 70 °C as well as the EVA/acetaminophen mix at 70 °C.

caused by physical interactions of the acetaminophen with the EVA excipient. While the present set of data does not provide a decisive conclusion, the benefit of the hyphenated Raman and rheology system to investigate complex morphology and phase behavior is apparent.

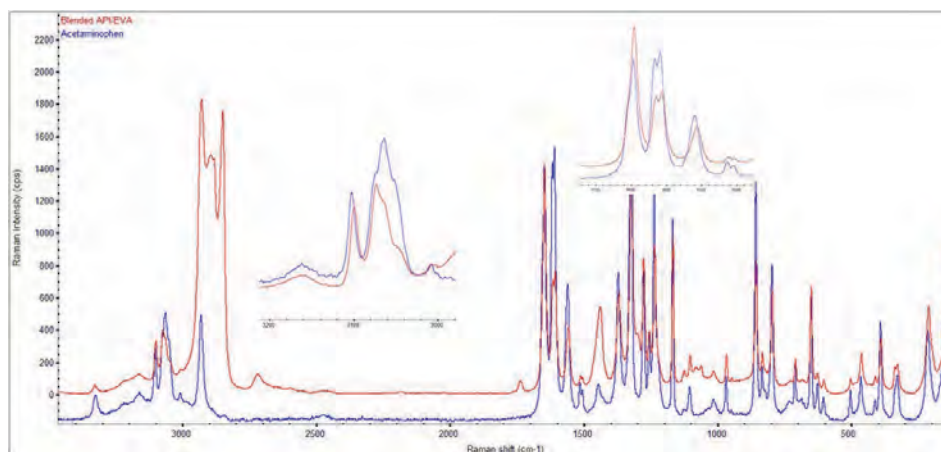


Fig. 8: Raman spectra of the pure acetaminophen (blue) and the EVA/acetaminophen mix after the rheological temperature ramp (red).

## Summary

It has been demonstrated that the HAAKE MARS<sub>XR</sub> hyphenated RheoRaman system can yield a wide range of relevant product parameters simultaneously. The neat EVA did not show a phase transition at 70 °C, whereas the EVA/acetaminophen mixture not only showed a phase transition but started the transition even earlier than the neat EVA at 65 °C. Acetaminophen acts as a nucleating agent during the isothermal crystallization of EVA, leading to a higher crystalline weight fraction in the EVA/acetaminophen mixture. The rheological results allow us to understand the viscoelastic behavior of the materials in a formulation process like HME, while also obtaining data about the morphology of the polymer and/ or API involved. The changes observed in the Raman spectrum for the acetaminophen before and after the temperature cycle are not fully understood yet. Further work will be necessary to allocate those changes to either a change in polymorph or to interactions with the EVA excipient.

## References

1. M. Richter, C. Schneider, "Low-Temperature Hot-Melt Extrusion of Acetaminophen with EVA", 2nd European Conference on Pharmaceutics, Krakow, 03 to 04 April 2017
2. Repka et.al., "Drug Development and Industrial Pharmacy", 33:909-926, 2007
3. Thermo Fisher Scientific Application note V286 "Rheology-Raman Spectroscopy: Tracking polymer crystallization with the combination of a rheometer and a Raman spectrometer", Jan P. Plog and Matthew Meyer

## Acknowledgement

The authors wish to thank the Celanese VitalDose® research team and particularly, Dr. Christian Schneider for the EVA materials and technical expertise provided. Also, many thanks to Dr. Margarethe Richter from Thermo Fisher Scientific in Karlsruhe for many fruitful discussions.

Find out more at [thermofisher.com/rheometers](https://thermofisher.com/rheometers) and [thermofisher.com/msr](https://thermofisher.com/msr)

**ThermoFisher**  
SCIENTIFIC

# Simultaneous rheology and Raman spectroscopy during the melting and recrystallization of polypropylene

**Authors:** Nathan C. Crawford and David Drapcho

## Introduction

Rheology is the study of the flow and deformation of matter, including fluids to solid-like materials (and anything in between). Rheological measurements are commonly used to examine or induce bulk physical material changes, such as melting, crystallization, gelation, and/or polymerization etc. Raman spectroscopy, on the other hand, is a vibrational spectroscopic technique that can provide insights to these processes at the molecular level, both chemically and morphologically. However, until very recently<sup>1</sup>, Raman studies are often conducted *ex-situ*, whereby Raman spectra are acquired prior to and after the observed physical transformation. The true chemical/morphological changes driving these processes are largely left uncaptured, leaving much room for data interpretation and speculation surrounding these dynamic physicochemical relationships.

The Thermo Scientific™ HAAKE™ MARSxR (Figure 1) is a fully integrated RheoRaman system that enables simultaneous rheology and Raman spectroscopy measurements. The seamless hyphenation of these two techniques allows for real-time, *in-situ* measurements of both physical and chemical/morphological properties with great ease. This multimodal analytical tool offers several advantages compared to the traditional *ex-situ* approach. First, data collection efficiency is greatly improved by combining multiple one dimensional experiments into a single multifaceted experiment. Secondly, because both techniques are employed simultaneously, sample fidelity is preserved and the transformation of the material is captured in real-time. And finally, sample consumption is reduced, which can be beneficial for new material/formulation development where sample quantities are limited and/or expensive.



**Figure 1:**  
The Thermo Scientific HAAKE MARSxR RheoRaman system.

In this note, a MARSxR RheoRaman system was used to investigate the temperature-dependent melting and crystallization of polypropylene, as well as the isothermal crystallization process. The melt and crystalline phase transitions of polymeric materials are commonly correlated with variations in viscous and elastic behavior during rheological analysis. In addition, these phase transitions are often associated with spectral pattern changes in characteristic Raman peaks during spectroscopic investigation. Measurements performed *ex-situ* are often challenging to compare due to discrepancies in temperature control, slight deviations in sample composition, and differences in processing history. The *in-situ* RheoRaman system, on the other hand, completely eliminates these discrepancies, allowing for a more valid analysis of the melt and crystalline phase transitions from both the macroscopic and molecular levels.

## Materials and methods

### Materials

Polypropylene (Ineos Olefins and Polymers, USA, R12C-00 random copolymer) pellets were used for this study. The pellets were melted at 190 °C on the rheometer to form a continuous, disk-shaped specimen for testing.

### Rheometer

Rheological measurements were performed using the Thermo Scientific™ HAAKE™ MARS™ III rheometer, equipped with a 20 mm diameter stainless steel parallel-plate rotor. In order to extract viscoelastic behavior of the polypropylene, all measurements were conducted in the oscillatory mode. Oscillatory measurements were performed at 1 Hz with a constant strain of 0.1%, while data were collected every 5 s. To soften the polypropylene and help it conform to the measuring geometry, all samples were initially loaded at 190 °C. For the melt-to-crystallization phase transition study, the temperature was decreased from 190 °C to 30 °C, at a rate of 5 °C/min. For the isothermal crystallization studies at 138 °C and 150 °C, temperature was rapidly decreased from 190 °C to 10 °C above the target temperature. The temperature was then slowly decreased until it reached the test temperature (either 138 °C or 150 °C). The temperature was then held constant for a maximum of 1 h (3600 s), while the isothermal recrystallization process was observed.

### Spectrometer

Raman spectroscopy measurements were performed using the Thermo Scientific™ iXR™ Raman Spectrometer. The iXR system employed a 532 nm, 10 mW laser, a triplet spectrograph providing Raman spectra over the range 3500 to 50  $\text{cm}^{-1}$  Raman shift (Stokes) at 5  $\text{cm}^{-1}$  resolution, and a CCD camera cooled to -50 °C. Alignment of the laser, Raman scatter, and aperture selection within the spectrometer were all software controlled. The minimum exposure collection time is 0.1 s. For the data presented here, the exposure collection time was 4 s and 2 sample exposures were averaged per spectra collection.

### RheoRaman coupling

The Raman spectrometer (Thermo Scientific iXR Raman Spectrometer) and rheometer (Thermo Scientific HAAKE MARS III) are coupled together using the Thermo Scientific™ HAAKE™ RheoScope module (Figure 2).

The iXR Raman spectrometer is free-space coupled to the rheometer with an optical train which uses two plane mirrors to direct the incident laser into the RheoScope module. Within the RheoScope, a series of mirrors directs the laser beam into a 20x objective, where the laser light is focused through a 2 mm thick fused silica window into the sample (perpendicularly to the flow or vorticity plane). Raman scattered light is collected in a 180° backscatter geometry using the 20x objective, and back into the spectrometer through the same optical train as the incident laser (eventually to the spectrograph inside the spectrometer). Free-space coupling of the laser to the rheometer, and the iXR spectrometer design, allow easy Raman excitation laser wavelength interchange to permit optimization of the laser wavelength to the sample (785 and 455 nm laser sets are also available).

The sample is positioned between the silica window and the rotor geometry attached to the rheometer measuring head (Figure 2). The objective can be adjusted for interrogation at different penetration depths within the sample, as well as positioned at various radial locations along the optical slit (from the true center to outer edge of the sample). An electrical heating element is positioned below the fused silica window to provide temperature control during testing. Cooling was provided from a temperature-controlled circulator with a 50:50 mixture of ethylene glycol and water. All instrumentation is controlled through the Thermo Scientific™ OMNIC™ and RheoWin software packages.

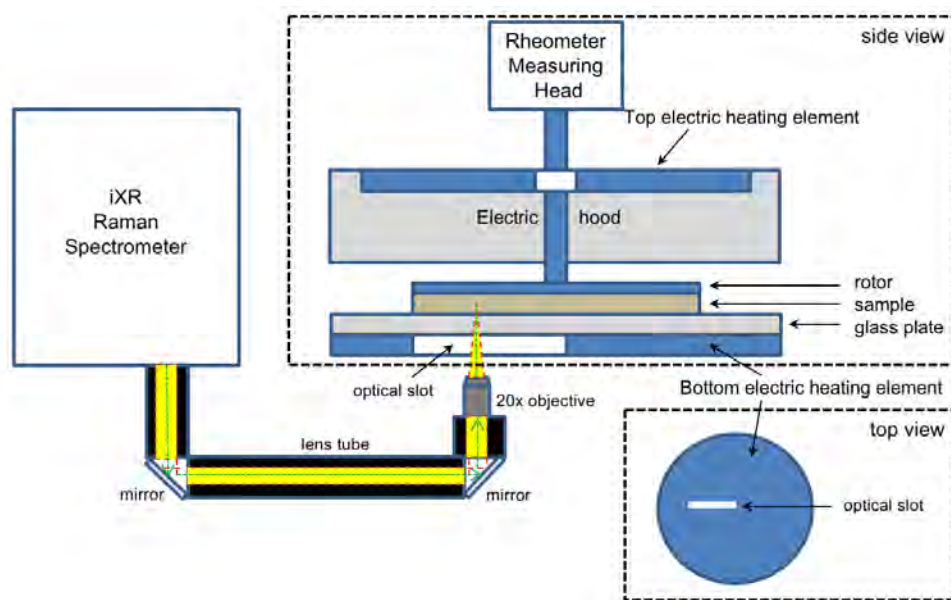


**Figure 2:** Schematic diagram of the MARS<sub>XR</sub> RheoRaman system (showing side and top views of the rheometer sample stage). The iXR Raman spectrometer is free-space coupled to the MARS rheometer using plane mirrors that direct light into a 20x long-working-distance objective. The objective focuses the incoming laser (green dashed line) and collects the back-scattered Raman light (yellow) coming into and out of the sample (which sits atop the rheometer stage). The optical path from the spectrometer to the rheometer is enclosed in lens tubes (black). The optical slot in the bottom heating plate permits passage of the laser beam and scattered Raman light.

The electric heater allows for a maximum temperature of 300 °C and a minimum temperature of -5 °C, with a maximum heating/cooling rate of 10 °C/min. An active electrical hood was also used to provide temperature control from above, eliminating the potential for a temperature gradient within the sample (Figure 2).

## Results and discussion

The physicochemical and morphological relationships during polymer crystallization are of critical importance for polymer processing. Here we use the new MARSxR RheoRaman system to investigate the crystallization process of polypropylene (PP). Representative Raman spectra for PP at three different temperatures are shown in Figure 3. In general, the spectrum at 53 °C shows sharp peaks across the examined spectral range. These sharp spectral features suggest a high degree of conformational order, indicative of semicrystalline and crystalline structures. As temperature increased to 120 and 173 °C, these peaks began to broaden and merge together. The broadening of spectral peaks is commonly ascribed to melt behavior in polymeric materials.

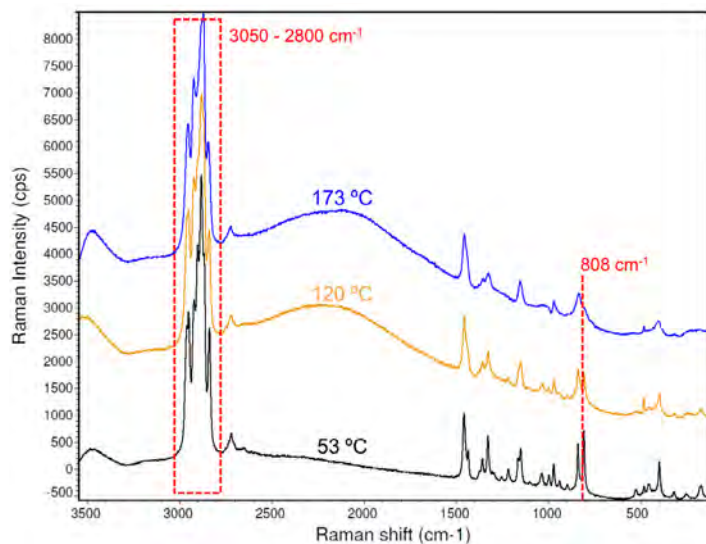


**Figure 3:** Raman spectra for polypropylene at 53 °C (black), 120 °C (yellow), and 173 °C (blue). The dashed line at 808 cm<sup>-1</sup> and dashed box from 3050-2800 cm<sup>-1</sup> indicate relevant Raman bands to the recrystallization of polypropylene.

Specific indicators in the Raman spectra for PP are the skeletal deformation of helical chains within the crystal (808 cm<sup>-1</sup> peak) and the CH stretching region (3050-2800 cm<sup>-1</sup> spectral range). The intensity of the 808 cm<sup>-1</sup> peak will be used as a measure of the crystallinity of PP<sup>2</sup>, and the intensity in the CH stretching region is used as a measure of the overall Raman scattering intensity during the crystallization process. For further analysis, the 808 cm<sup>-1</sup> peak height was normalized by the peak area between 880 and 780 cm<sup>-1</sup>. The 880-780 cm<sup>-1</sup> spectral region contains skeletal chain vibrations of all conformations during the

melt-to-recrystallization process<sup>2</sup>, while the spectral features in the 3050-2800 cm<sup>-1</sup> range were integrated into a total peak area. These indicators (normalized helical chain vibration peak height and overall CH stretching peak area) were then tracked throughout the melt- to crystalline-phase transition and overlaid with the in-situ rheology data (Figure 4).

The melt and recrystallization process of polypropylene was probed rheologically using small amplitude oscillatory shear measurements (Figure 4), where the storage modulus (G') and loss modulus (G'') were measured as a function of temperature. G' and G'' are measures of a material's elastic and viscous behavior, respectively. A liquid-like material will be more viscous than elastic (i.e., viscously dominated), and as a result, G'' will be greater than G'. Conversely, a solid-like material will display more elastic than viscous behavior (i.e., elastically dominated), where G' will be greater than G''.

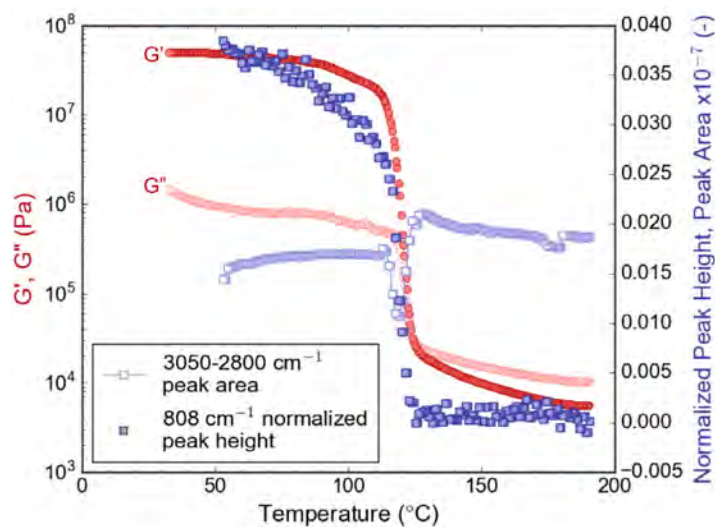


**Figure 4:** Polypropylene recrystallization: G' and G'' (filled and open circles, respectively; plotted on the left y-axis) and the normalized 808 cm<sup>-1</sup> Raman shift peak height and the 3050-2800 cm<sup>-1</sup> peak area (filled and open squares, respectively; plotted on the right y-axis) as a function of decreasing temperature from 190 to 30 °C.

Initially, at high temperatures (>150 °C), G'' was consistently greater than G', indicating the PP specimen was in the melt state and displaying liquid-like behavior. As the temperature decreased from 150 °C to 100 °C, an abrupt and drastic increase in both G' and G'' was observed at ~125 °C. By the time the temperature reached 100 °C, G' had increased by four orders of magnitude, while G'' increased by two orders of magnitude. The temperature range from 150 to 100 °C can be viewed as the melt-to-crystalline transition region for this polypropylene material. As the temperature further decreased to below 100 °C, G' was significantly greater than G'' by more than a full order of magnitude, indicating the polypropylene had transitioned into the semicrystalline and/or crystalline state, and was exhibiting solid-like behavior.

The observed plateau regions and increase in  $G'$  and  $G''$  are in direct agreement with the Raman spectral data (Figure 4). In the melt region ( $\sim 190$ - $130$  °C)<sup>-1</sup>, the normalized  $808$   $\text{cm}^{-1}$  peak height was near zero and remained unchanged by the decreasing temperature. However, as the PP melt began to crystallize, the normalized  $808$   $\text{cm}^{-1}$  peak height significantly increased and was in unison with the abrupt increases in both  $G'$  and  $G''$ . Also, as the PP sample started to crystallize, the total peak area of the CH stretching region decreased rapidly before any measurable growth of the  $808$   $\text{cm}^{-1}$  band was observed. The decrease in intensity in the  $3050$ - $2800$   $\text{cm}^{-1}$  spectral region is postulated to be caused by the formation of crystallites in the PP matrix. Crystallites with dimensions on the same order of magnitude as the wavelength of the incident laser ( $532$  nm) would scatter light, thereby creating a loss in the Raman signal intensity of the CH stretching bands. The minimum in the CH stretching profile was directly aligned with the observed crossover between  $G'$  and  $G''$  and the maximum slope of the normalized  $808$   $\text{cm}^{-1}$  peak profile. The correlation between changes in the Raman spectral features and the rheological response indicate that the crystallization rate was at its maximum when the crystallite concentration was greatest. After the observed decrease in intensity, the integrated area of the CH stretching region returned to a value close to what was detected in the melt phase.

In order to further evaluate the crystallization process of PP, isothermal crystallization studies were performed at  $150$  and  $138$  °C. The PP samples were heated at a minimum of  $5$  min at  $190$  °C (to fully melt the specimen), rapidly cooled at  $10$  °C /min to  $10$  °C above the crystallization temperature, and then cooled at a slower rate of  $2$  °C /min until the set crystallization temperature was reached. The crystallization temperature was then held constant for a maximum of  $1$  h ( $3600$  s) to observe the isothermal crystallization of PP as a function of time. Simultaneous rheology and Raman spectroscopy data were acquired in-situ during crystallization at  $138$  and  $150$  °C (Figures 5 and 6, respectively). At both isothermal temperatures, the PP material was initially viscously dominated  $G' < G''$  displaying liquid-like behavior. As time progressed, a crossover in  $G'$  and  $G''$  was observed; where the moduli increased 2 to 3 orders of magnitude. The crossover at  $138$  °C occurred at  $84$  s into the isothermal curing process, while it took  $2150$  s for the crossover to be observed at  $150$  °C. After the observed crossover,  $G'$  and  $G''$  reached a plateau and the crystallization process was considered stabilized and complete.

Similar to the previous experiments, the rheology and Raman data were in agreement during the isothermal crystallization studies (Figures 5 and 6). The observed increase in the elastic and viscous moduli directly correlates with the increase in the normalized  $808$   $\text{cm}^{-1}$  peak height. Although not shown here, a minimum in the CH stretching band intensity was again observed as the specimen transitioned from the liquid to the solid state.

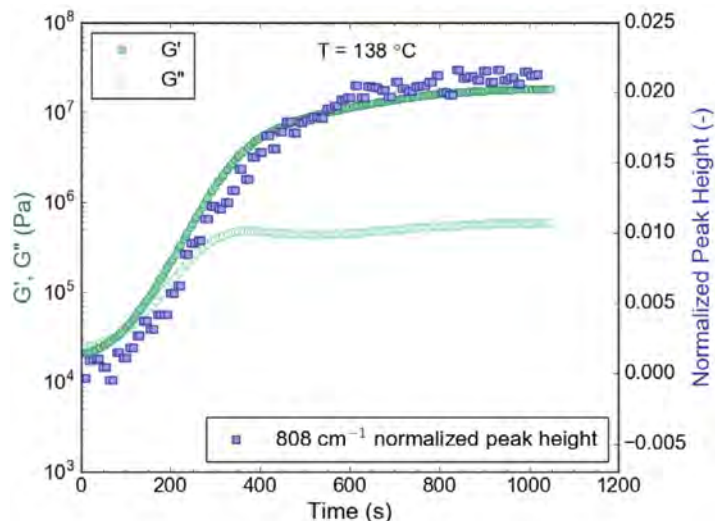


**Figure 5:** Polypropylene isothermal recrystallization at  $138$  °C :  $G'$  and  $G''$  (filled and open circles, respectively; plotted on the left y-axis) and the normalized  $808$   $\text{cm}^{-1}$  Raman shift peak height (filled squares; plotted on the right y-axis) as a function of time.

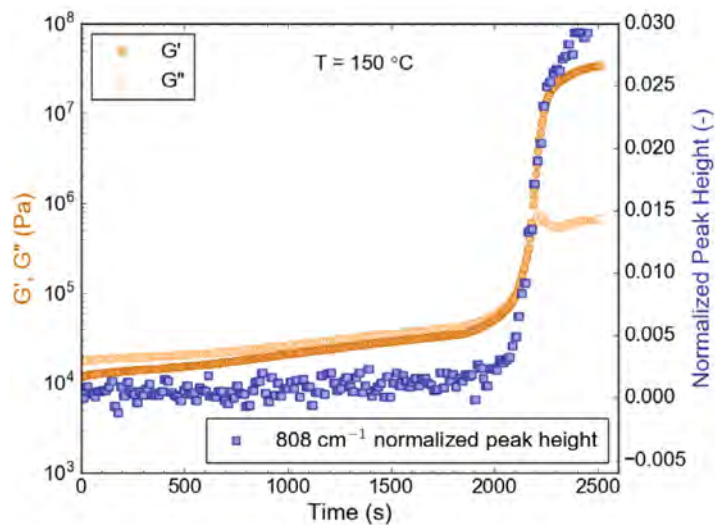


**Figure 6:** Polypropylene isothermal recrystallization at  $150$  °C :  $G'$  and  $G''$  (filled and open circles, respectively; plotted on the left y-axis) and the normalized  $808$   $\text{cm}^{-1}$  Raman shift peak height (filled squares; plotted on the right y-axis) as a function of time.

## Conclusions

A MARS<sub>XR</sub> system was employed to simultaneously measure the rheology and Raman spectroscopy of polypropylene during the melt-to-crystallization transition process. This multimodal analytical tool allowed the bulk structural properties of polypropylene ( $G'$  and  $G''$ ) to be directly correlated with conformational changes at the molecular level (helical chain vibrations and CH stretching) in real-time. The data revealed that the rate of crystallization reached its maximum (indicated by rapid increases in  $G'$ ,  $G''$ , and the normalized  $808\text{ cm}^{-1}$  peak height) when the crystallite concentration was greatest (signified by a decrease in the overall Raman spectral intensity in the  $3050\text{-}2800\text{ cm}^{-1}$  region). The observed correlation between the macroscopic and molecular level measurements exemplifies the unique analytical capability unleashed by hyphenating rheology with Raman spectroscopy. While this work focusses on the melting and crystallization of PP, the underlying principles demonstrated here should be applicable for a wide range of material processes including gelation, polymerization, curing behavior, as well as other shear-induced phenomena.

## References

1. A.P. Kotula, M.W. Meyer, F. De Vito, J. Plog, A.R. Hight Walker and K.B. Migler, Review of Scientific Instruments, 87, 105105 (2016); DOI 10.1063/1.4903746.
2. R.A. Khafagy, Journal of Polymer Science: Part B: Polymer Physics, DOI 10.1002/polb

Find out more at [thermofisher.com/mars](http://thermofisher.com/mars)

**ThermoFisher**  
SCIENTIFIC

# Investigating cocoa butter crystallization using simultaneous rheology and Raman spectroscopy (RheoRaman)

## Author

Nathan C. Crawford and  
Mohammed Ibrahim  
Thermo Fisher Scientific  
Madison WI, USA

## Keywords

Cocoa butter, crystallization, Raman spectroscopy, rheology, RheoRaman, *in situ*, storage modulus  $G'$ , loss modulus  $G''$

## Thermo Fisher Scientific solutions

- HAAKE MARS 60 rheometer
- iXR Raman Spectrometer
- HAAKE RheoRaman module
- OMNIC for Dispersive Raman software

## Application benefits

Simultaneous rheology and Raman spectroscopy measurements were used to examine the isothermal crystallization of cocoa butter (CB). The results indicate that CB crystallized by first hardening into an amorphous solid. The amorphous solid then underwent a morphological transition to form a crystalline solid. Without coupling these two separate analytical techniques, the observed amorphous-solid to crystalline-solid transformation would have been left undetected. Alone, each technique suggests a single-stage process, however, only when the two techniques are coupled is the multi-phase crystallization process revealed, further exemplifying the unique analytical capability unleashed by hyphenating rheology with *in situ* Raman spectroscopy.

## Introduction

Cocoa butter (CB) is an edible vegetable fat extracted from the cocoa bean. CB is commonly used in home and personal care products (such as ointments and lotions) and CB is a vital ingredient in chocolate. CB forms the continuous phase within chocolate confections and is responsible for the chocolate's texture, snap, gloss, melting behavior, and resistance to fat bloom. These physical characteristics are a direct result of CB's triacylglycerol (TAG) composition and overall crystalline structure.

In general, TAG molecules assume a tuning fork configuration and the TAG "forks" assemble to form crystal lattice structures. During crystallization, the TAG molecules slow down as the CB oil cools and the TAGs come to rest in contact with one another, forming what are known as "sub crystalline cells."<sup>1</sup> Once the sub-cells are formed, they are thermodynamically driven to aggregate into larger and more stable crystalline structures.<sup>2</sup> The self-assembly of sub-cell structures and their further aggregation is governed by a balance of intra- and inter-molecular interactions. Depending on the molecular level packing and orientation of the TAGs, CB can form different types of crystal lattice structures (or polymorphs), where some crystal structures are more desirable than others. Overall, CB crystallization is a highly complex, multistage process. Understanding the isothermal crystallization behavior of CB is vital for improving chocolate manufacturing processes and maintaining product quality.

In this note, rheology coupled with *in situ* Raman spectroscopy was used to examine the isothermal crystallization of cocoa butter. Raman spectroscopy is a highly sensitive, relatively fast, and nondestructive technique that can probe the molecular structure and conformation in both liquid and solid TAG assemblies, as well as intra- and inter-TAG interactions. With simultaneous Raman spectra and rheological data, molecular-level interactions and conformational shifts during the isothermal crystallization of CB were directly correlated with the changes in bulk viscoelastic properties, providing unique insight into the multifaceted crystallization behavior of cocoa butter.

## Materials and methods

### Materials

Commercially available, organic cocoa butter (*Theobroma cacao*) was acquired from Inesscents™ (Ashland, OR, USA).

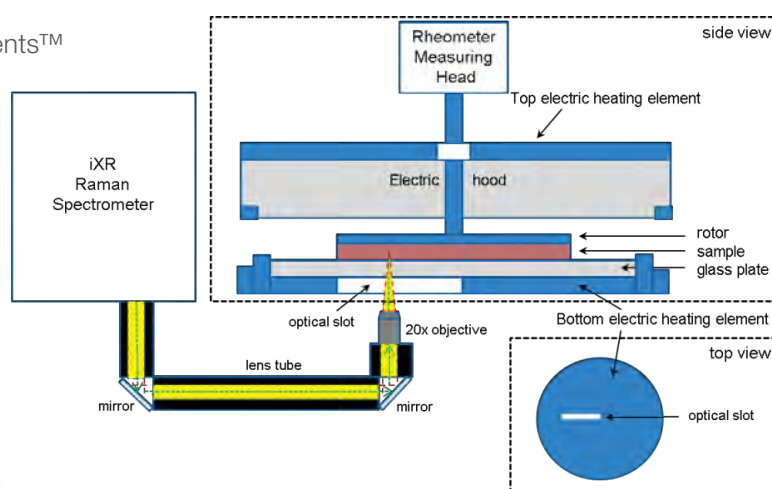


**Figure 1. (a)** The Thermo Scientific™ HAAKE™ MARSxR RheoRaman System. **(b)** Schematic diagram of the MARSxR RheoRaman system (showing side and top views of the rheometer sample stage). The iXR Raman spectrometer is free-space coupled to the MARS rheometer using lens tubes and mirrors that direct light into a 20x objective. The objective focuses the incoming laser (green dashed line) and collects the back-scattered Raman light (yellow) coming out of the sample sitting atop the rheometer stage.

### Raman spectroscopy

Raman spectroscopy measurements were performed using a Thermo Scientific™ iXR™ Raman Spectrometer. A 532 nm laser was used with 10 mW laser power at the sample. The spectral range was 50-3500  $\text{cm}^{-1}$ . The spectra were collected using a 2-second exposure time and 4 sample exposures. Data acquisition and processing were controlled by the Thermo Scientific™ OMNIC™ Software for Dispersive Raman. For the data presented here, Sequential Raman spectra (in parallel with the Rheological measurements) were collected over a predetermined time window using the time series collection function of the SERIES software within the OMNIC for Dispersive Raman software package.

### Rheology

Rheological measurements were performed using a Thermo Scientific™ HAAKE™ MARS™ 60 Rheometer equipped with a serrated 35 mm diameter plate rotor at a gap height of 1 mm. The serrated plate was used to prevent slip at the sample-rotor interface. All measurements were conducted in the oscillatory mode, with a frequency of 1 Hz and a constant strain of 0.1%. CB samples were loaded onto the rheometer at 60 °C and allowed to equilibrate for 10 min to erase any crystal structures and/or shear history from sample loading. After the equilibrium step, the temperature was rapidly decreased from 60 °C to 22 °C at a rate of 10 °C/min. The temperature was then held constant at 22 °C for 120 min, collecting data every 10 s.

### RheoRaman coupling

The Thermo Scientific™ HAAKE™ MARSxR RheoRaman System consists of the iXR Raman spectrometer and the HAAKE MARS 60 rheometer coupled together using the HAAKE RheoRaman module (Figure 1a). The iXR Raman spectrometer was free-space coupled to the rheometer with an optical train which used a series of mirrors to direct the incident laser into the RheoRaman module (Figure 1b). Within the module, a mirror directed the laser beam into a 20x objective, where the laser light was focused into the sample (perpendicularly to the flow or vorticity plane). Backscattered Raman light was collected using the same 20x objective and guided back to the spectrometer using the same optical train as the incident laser (eventually to the spectrograph inside the spectrometer; Figure 1b).

The sample was positioned between a sandblasted glass bottom plate and the serrated 35 mm plate rotor (the textured plates were used to avoid slip at the sample-plate interfaces). An electrical heating element within the RheoRaman module provided temperature control from below the sample, while an active electrical hood was used to provide temperature control from above (eliminating the potential for a temperature gradient within the sample). Cooling of the sample was supplied from a temperature-controlled water bath circulator.

## Results and discussion

### Raman spectroscopy: Cocoa butter crystallization

Raman spectra for the liquid phase CB melt and the crystalline solid CB in the 500-3100  $\text{cm}^{-1}$  range are shown in Figure 2. Prominent Raman features were observed in both the C-H stretching region (2700-3050  $\text{cm}^{-1}$ ) and the fingerprint region (1000-1800  $\text{cm}^{-1}$ ). More specifically, the lower Raman shift features include: the carbonyl (C=O)

stretching region (1700-1800  $\text{cm}^{-1}$ ), the olefinic (C=C) band at  $\sim 1655 \text{ cm}^{-1}$ , the  $\text{CH}_3$  and  $\text{CH}_2$  deformations ( $\sim 1460$  and  $1440 \text{ cm}^{-1}$ , respectively), the  $\text{CH}_2$  twisting region (1250-1300  $\text{cm}^{-1}$ ), and the C-C stretching region (1000-1200  $\text{cm}^{-1}$ ).

The C-H stretching regions for the melted and solidified CB specimens are highlighted in Figure 3. Two strong peaks were observed at  $\sim 2850 \text{ cm}^{-1}$  and  $2882 \text{ cm}^{-1}$ , which are attributed to symmetric and asymmetric  $\text{CH}_2$  stretching, respectively.<sup>2</sup> The symmetric vibrational modes at  $2850 \text{ cm}^{-1}$  were dominant in the liquid (melt) phase, while the asymmetric vibrations at  $2882 \text{ cm}^{-1}$  were dominant in the solid phase. Thus, the  $2850 \text{ cm}^{-1}$  and  $2882 \text{ cm}^{-1}$  bands are strong indicators of amorphous and crystalline content, respectively.<sup>3</sup> Subsequently, the  $I_{2882}/I_{2850}$  peak intensity ratio was used to dynamically track crystal formation during the *in situ* RheoRaman measurements.

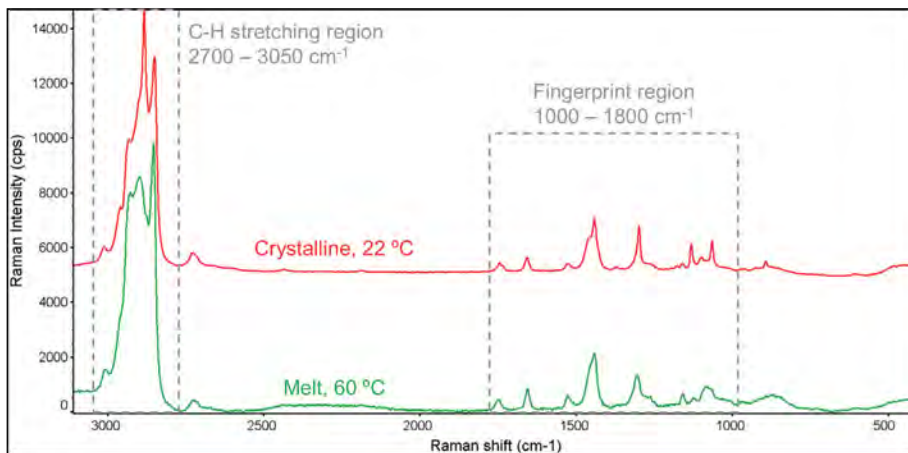
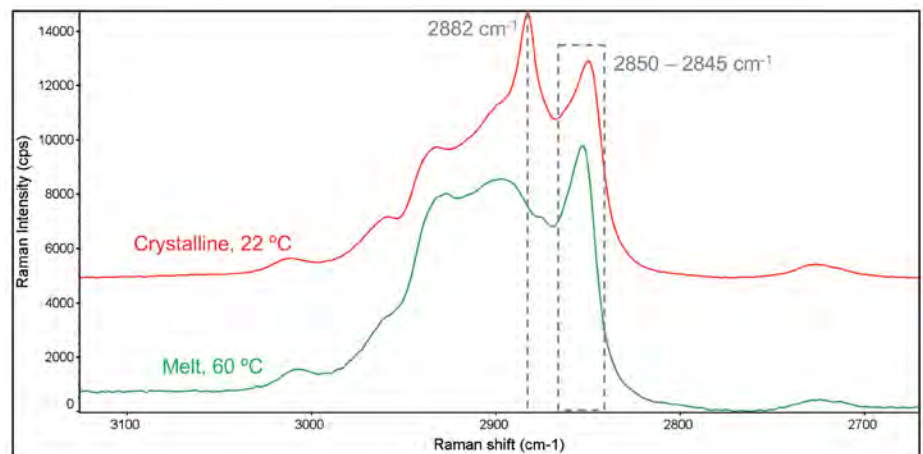


**Figure 2.** The full Raman spectra of melted and crystalline cocoa butter.

**Figure 3.** Raman spectra of the C-H stretching region (2700-3050  $\text{cm}^{-1}$ ) for melted and crystalline cocoa butter.



Although less intense than the C-H stretching region, approximately eight unique spectral features were identified in the fingerprint region (1000-1800  $\text{cm}^{-1}$ ; Figure 4). When comparing the CB melt state to the crystalline phase, the most significant changes were observed in the C-C stretching region (1000-1200  $\text{cm}^{-1}$ ).

Two well-defined features emerged at  $1130 \text{ cm}^{-1}$  and  $1063 \text{ cm}^{-1}$  during the solidification process, which originate from the symmetric and asymmetric C-C stretching, respectively.<sup>4,5</sup> In the melt phase, all C-C stretching bands were relatively weak and broad due to the disordering effects of methyl gauche conformations.

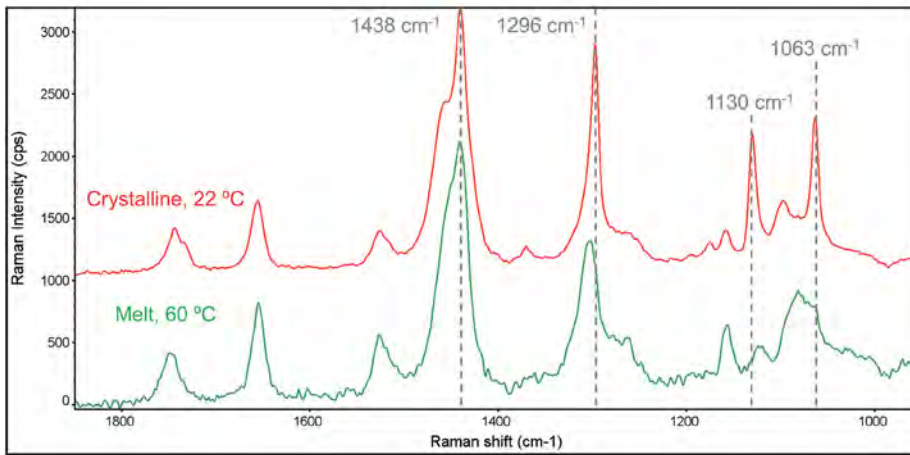


**Figure 4.** The 1000–1800  $\text{cm}^{-1}$  Raman spectral range for melted and crystalline cocoa butter.

However, as the CB solidified, the backbone methyl groups were ordered into the trans-conformation, signified by the emergence of the peak at  $1130\text{ cm}^{-1}$ . Therefore, in addition to the  $I_{2882}/I_{2850}$  peak intensity ratio, the  $I_{1130}/I_{2850}$  spectral marker was also used to track the crystalline-phase transition within CB via *in situ* rheoRaman measurements.

### **Simultaneous rheology and Raman spectroscopy (RheoRaman)**

The melt-to-solid phase transition of cocoa butter was probed rheologically using small amplitude oscillatory shear measurements (Figure 5a), where the storage modulus  $G'$  and loss modulus  $G''$  were measured as a function of time at the isothermal temperature of  $22\text{ }^{\circ}\text{C}$ .  $G'$  and  $G''$  are measures of a material's elastic and viscous behavior, respectively. A liquid-like material will be more viscous than elastic (i.e., viscously dominated), and as a result,  $G''$  will be greater than  $G'$ . Conversely, a solid-like material will display more elastic than viscous behavior (i.e., elastically dominated), where  $G'$  will be greater than  $G''$ . The overall magnitudes of  $G'$  and  $G''$ , as well as their relative difference in magnitude, often reported as the ratio of  $G''/G'$ , determines the general viscoelasticity and overall resistance to deformation for a given material.

The ratio of  $G''/G'$  (plotted on the right y-axis of Figure 5a) is commonly used to track viscoelasticity of a material:

$$\frac{G''}{G'} = \tan(\delta),$$

where  $\delta$  is the phase angle defined as the shift or lag between the input strain and resultant stress sine waves (or vice versa) during an oscillatory shear measurement. The term “ $\tan(\delta)$ ” is often referred to as the loss or damping factor. Values of  $\tan(\delta)$  less than unity indicate elastically dominant (solid-like) behavior, while values greater than unity indicate viscously dominant (liquid-like) behavior.

Unlike the individual moduli,  $\tan(\delta)$  can be used to quantify overall brittleness of a material and is commonly used to assess glass transition behavior. In general, as  $\tan(\delta)$  becomes smaller, the more  $G'$  deviates from  $G''$ , and the more brittle (or glass-like) the material becomes.

During the initial portion of the isothermal hold at  $22\text{ }^{\circ}\text{C}$  from 0 to 5 min (immediately following the rapid decrease in temperature from  $60\text{ }^{\circ}\text{C}$  to  $22\text{ }^{\circ}\text{C}$ ), both  $G'$  and  $G''$  increased as the CB transformed from a melted liquid to a soft semi-solid (Figure 5a). This initial increase in modulus is most likely due to a delay between the set temperature and the internal temperature of the loaded sample. Once the sample had reached thermal equilibrium and was at the isothermal set point of  $22\text{ }^{\circ}\text{C}$ , the moduli were relatively stable from 10 to 25 min. From 25 to 50 min, however, both  $G'$  and  $G''$  begin to gradually increase and then from 50 to 80 min, the moduli rapidly increased, where  $G'$  and  $G''$  increased by approximately 5 and 4 orders of magnitude, respectively. The exponential increase in the moduli indicates a solidification process, where the CB transformed from a pliable semi-solid to a more robust, hardened solid. At 80 min and beyond, growth in the elastic modulus slowed and eventually plateaued, showing no further significant change past 100 min. The viscous modulus, however, reached a slight plateau from 80 to 100 min and then proceeded to gradually decrease from 100 min and beyond.

During the increase in  $G'$  and  $G''$ , a rapid decrease in the loss factor  $\tan(\delta)$  was observed from  $\sim 65$  min and beyond (Figure 5a, right y-axis). The decrease in the loss factor indicates a deviation in overall magnitude between  $G'$  and  $G''$ . As the CB hardened, the increase in  $G'$  exceeded the increase in  $G''$ , triggering the decrease in  $\tan(\delta)$ . At the end of the 120 min isothermal study,  $G'$  was more than a full order of magnitude greater than  $G''$  and the loss factor was approaching 0.01, indicating the CB had transitioned into a brittle glass-like solid.

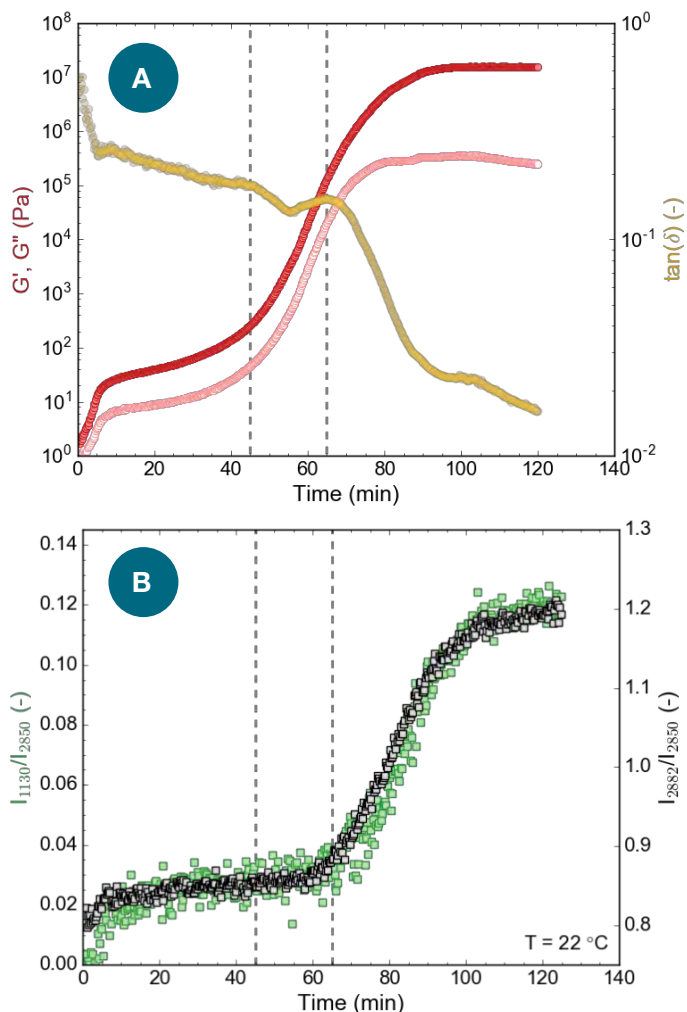


**Figure 5. (a)** Rheology:  $G'$  and  $G''$  (filled and open circles, respectively; plotted on the left y-axis) and  $\tan(\delta)$  (plotted on the right y-axis) and **(b)** Raman: the  $I_{1130}/I_{2850}$  (left y-axis, green) and  $I_{2882}/I_{2850}$  (right y-axis, black) peak intensity ratios for CB during isothermal crystallization at 22 °C. The vertical dashed line at 45 min indicates the increase of  $G'$  and  $G''$ , while the dashed line at 65 min indicates the decrease in  $\tan(\delta)$  and increase in the Raman ratios.

The observed rheological behavior was further confirmed using simultaneous Raman spectroscopy (Figure 5b). Initially, both the  $I_{1130}/I_{2850}$  and  $I_{2882}/I_{2850}$  peak intensity ratios remained unchanged during the first ~65 min of the isothermal study. Then a sharp increase of the  $I_{1130}/I_{2850}$  and  $I_{2882}/I_{2850}$  ratios began at ~65 min, indicating the formation of crystal structures within the CB. As the CB further crystallized, both spectral markers continued to increase from 65 to 100 min. Beyond 100 min, the growth in both Raman features had subsided and the peak intensity ratios began to stabilize.

Overall, the rate of increase in the 1130 and 2882  $\text{cm}^{-1}$  spectral ratios were similar to the rate of change for both  $G'$  and  $G''$  (i.e., they increased with similar slopes). However, there was a noticeable 15-20 min lag between the observed increase in  $G'$  and  $G''$  and the rise of the Raman intensity ratios. The sharp upturn in  $G'$  and  $G''$  indicates an increased resistance to deformation (i.e., a bulk hardening of the CB), signaling the start of the solidification process. The

Raman spectral markers, on the other hand, are indicators of crystal formation. Thus, the time delay between the rheology and Raman profiles suggests that CB first hardens into an amorphous solid, followed by a transformation from an amorphous to a crystalline solid. This morphological transformation was signified by the subsequent increase in the Raman band intensities associated with crystal CB structures (the 1130 and 2882  $\text{cm}^{-1}$  peaks). The temporal separation of the rheological and Raman spectral profiles indicates a clear distinction between bulk hardening of the CB and the formation of crystalline domains.

Interestingly, the increase in the Raman spectral features ( $I_{1130}/I_{2850}$  and  $I_{2882}/I_{2850}$ ) directly correlated with the observed reduction in  $\tan(\delta)$  (Figure 5a and b). The loss factor is an indication of material brittleness and crystalline structures are commonly known to be brittle. Thus, it is reasonable that the formation of crystal domains at the molecular level (as indicated by Raman) coincides with the overall brittleness of the CB. As a result, the loss factor may be a more revealing indicator of bulk CB crystallization than  $G'$  and  $G''$  alone.

## Conclusions

Simultaneous rheology and Raman spectroscopy measurements were used to examine the isothermal crystallization of cocoa butter. This multimodal analytical technique allowed the bulk mechanical properties of cocoa butter ( $G'$ ,  $G''$ , and  $\tan(\delta)$ ) to be directly correlated with conformational changes at the molecular level ( $\nu_{\text{as}}(\text{CH}_2)$  mode at 2882  $\text{cm}^{-1}$  and the  $\nu_{\text{s}}(\text{C-C})$  mode at 1130  $\text{cm}^{-1}$ ) in real-time. After rapid cooling (10 °C /min) and at an isothermal temperature of 22 °C, there was a noticeable time lag between the rheological response ( $G'$  and  $G''$ ) and the Raman spectral profiles. The observed time delay indicates that CB crystallized by first hardening into an amorphous solid, manifested by a sharp increase in  $G'$  and  $G''$  while the Raman features remained unchanged. The amorphous solid then underwent a morphological transition to form a crystalline solid, signified by the increase in Raman features associated with crystal CB structures (1130 and 2882  $\text{cm}^{-1}$ ). Without coupling these two separate analytical techniques, the observed amorphous-solid to crystalline-solid transformation would have been left undetected. Alone, each technique suggests a single-stage process, however, only when the two techniques are coupled is the multi-phase crystallization process revealed, further exemplifying the unique analytical capability unleashed by hyphenating rheology with *in situ* Raman spectroscopy. While this work focusses on the isothermal crystallization of CB, the underlying principles applied here should be applicable for a wide range of material processes including gelation, polymerization, curing behavior, as well as other shear-induced phenomena.

## References

1. K. Sato, *Crystallization of Lipids: Fundamentals and Applications in Food, Cosmetics, and Pharmaceuticals*. Hoboken, NJ: John Wiley & Sons, 2018.
2. S. Bresson, D. Rousseau, S. Ghosh, M. El Marssi, and V. Faivre, *Raman spectroscopy of the polymorphic forms and liquid state of cocoa butter*, Eur. J. Lipid Sci. Technol. 113, 992–1004, 2011.
3. R. G. Snyder, H. L. Strauss, and C. A. Elliger, *C–H stretching modes and the structure of n-alkyl chains*. 1. Long, disordered chains, J. Phys. Chem. 86, 5145–5150, 1982.
4. R. J. Meier, *Studying the length of trans conformational sequences in polyethylene using Raman spectroscopy: A computational study*, Polymer. 43, 517–522, 2002.
5. M. Zheng and M. Du, *Phase behavior, conformations, thermodynamic properties, and molecular motion of multicomponent paraffin waxes: A Raman spectroscopy study*. Vib. Spectrosc. 40, 219–224, 2006.

Find out more at

[www.thermofisher.com/Raman](http://www.thermofisher.com/Raman)

[www.thermofisher.com/MARS](http://www.thermofisher.com/MARS)

**ThermoFisher**  
SCIENTIFIC

## Customer service

We are committed to delivering top-notch customer support, including tailored service products and fast response times. We offer a comprehensive range of services that can quickly and flexibly respond to various service needs and requests.

## Application laboratories and support

Our fully equipped application laboratories are in constant demand for testing customer samples, and developing and optimizing pioneering applications. We also provide a broad range of product and application solutions, and our team of application specialists is on hand to answer your questions.

## Seminars, training courses and webinars

You will find comprehensive training programs, in-house seminars, and practical courses for extrusion, spectroscopy and rheology in various locations around the world.

Register for application and product information at [thermofisher.com/specoptin](https://thermofisher.com/specoptin) to gain access to latest resources to accelerate your research and improve laboratory productivity.

Find out more at

[thermofisher.com/materialcharacterization](https://thermofisher.com/materialcharacterization)

[thermofisher.com/rheology](https://thermofisher.com/rheology)

[thermofisher.com/spectroscopy](https://thermofisher.com/spectroscopy)

**ThermoFisher**  
SCIENTIFIC